Università Ca'Foscari Venezia

Master's Degree

in Conservation Science
and Technology for
Cultural Heritage

Final Thesis

Concotto artefacts from the Etruscan settlements of Adria and San Basilio di Ariano nel Polesine

Supervisor
Prof. Elisabetta Zendri
Dr Alberta Facchi

Assistant supervisor
Dafne Cimino, PhD

Graduand
Margherita Cantelli
Matricolation number
854492

Academic Year
2018 / 2019

Index

AIM OF THE STUDY

Aim of the study is the characterisation of non-vascular ceramic materials from two distinct Etruscan settlements situated in the Po Delta region (north Italy). One excavation took place in 1983 in the village of San Basilio di Ariano nel Polesine (Rovigo), and the other one in 2016 in the small town of Adria (Rovigo).

These archaeological findings are supposed to be building materials used for covering house walls, as external or internal plasters. Almost all of them have a smooth surface, going from red to light grey, and an opposite face that differs in texture as well as in colour. Notable details are the presence of one or more imprint on the smoothest face, probably due to the impression of thin plant elements, and the presence of some fingerprints on the edges, representing signs of the working process. Few pieces are characterised by a twisted decoration pattern. In addition, several portions of clay found in San Basilio site are characterized by reeds and branches prints, suggesting the *incannucciato* technique for the realization.

Similar materials were found also during the excavation in the shore of Spina (Ferrara). Publications about findings from this site describe walls coated by a system of clay slabs, trimmed and painted on a side, with the constant feature of a defined layer of *ingobbio*. Due to the co-presence of plasters and *incannucciato*, a mixed building technique has been suggested: plaster used in the bottom part of the wall being more water-resistant, and raw clay to cover the upper part of the vegetable structure (Zamboni, 2016).

In this study a set of samples was analysed by means of a multi-analytical approach: Fourier-transform infrared (FTIR) and FTIR in Attenuated Total Reflection (ATR) mode spectroscopies, thermogravimetry coupled with differential scanning calorimetry (TGA-DSC), stereo-microscopic analyses of cross sections and evaluation of the open porosity. This approach allowed to underline similarities and differences about the composition of ceramic mixtures and possible coatings, as well as the methodology of firing technique.

The expectation is to clarify the role of this ceramic materials, in order to better understand the construction process that appears unique for San Basilio, Adria and Spina settlements.

1. INTRODUCTION

1.1 Etruscan civilization in the Po Valley

Etruscans were a civilization of ancient Italy whose origins are still unclear. Different theories have been developed about the provenience of the Etruscan people from various regions, but the more considered ones brought Etruscans from east-central Europe (Camporeale, 1997; Torelli, 1981).

What is historically known is that this civilization covered a wide period of time, from the 9th to the 1st century BC, establishing in territories in the area defined by the Tyrrhenian Sea on the west, the Arno river on the north and the Tiber on the south-east, adding the etruscanized areas of Emilia-Romagna and the Po Valley on the north, and the Campania region on the south (Figure 1).

Firstly, it is useful to recognise the different stages of Etruscan settlements from the beginning, in order to understand the colonization concerning the Po plain area.

Archaeology reveals a clear cultural continuity between the Bronze Age and the

Figure 1. Etruscans territory (Zanichelli, s.d.).

Iron Age in the territory of historical Etruria, without any signs of invasions or migrations.

During the Bronze Age (2nd millennium BC), the peninsular area of Italy was characterized by a specific homogeneous culture, named Apennine for the close correlation with the mountain range (the Apennines) crossing the territory from the Emilian slopes to the very end of Calabria. The main economic activity of this culture consisted in sheep farming with transhumance practices. Moreover, agriculture was the principal feed source and breeding started to become important also for wool and cheese production. Apennine populations produced fine ceramic with a dark body composed of non-purified clay, decorated with carved lines and dots forming a continuous design filled with white and ochre dyes.

The first signs of transformation appeared to be in the late Bronze Age (13th century BC), with the disappearance of the carved decoration on pottery. However, it is in the latest Bronze Age periods that radical changes occurred, both cultural and archaeological, named as Sub-Apennine and Proto-Villanovan populations. Sub-Apennine settlements were the natural extension of those from the previous Apennine culture, even if new open villages were established on the hills. Furthermore, ceramic artefacts displayed some changes, such as the definitive abandonment of carved decorations

and the addition of some appendices and handles. The great innovation involved the bronze industry, forging new types of weapons and artefacts for personal use taking inspiration from the Middle-Europe. On the other hand, Proto-Villanovan culture presented some radical changes: previous open settlements appeared surrounded by defensive stone fences showing a more stable character and tribal organizations turned into different configurations, forming wide households and introducing the private possession of lands. Concerning pottery production, ceramic bodies became rougher and vases presented less decorations. An important revolution regarded the cult of dead: with the introduction of body cremation large necropolis appeared and ashes were buried in biconical urns with few funerary objects. However, in the 10th century BC, cremations appeared to have burial goods that distinguished social status through weaponry: some miniatures of bronze weapons were introduced in the grave offerings of male adults, as a consequence of the emerging warrior culture. The largest numbers of Proto-Villanovan settlements were found in the north Tuscan area, which would become the southern Etruria.

New local cultures established between the 10th and the 9th century BC, defining their characters, such as the Villanovan population, becoming the core of the Etruscan culture in history. Moreover, this is considered as the most ancient phase of the Etruscan civilization. Settlements grew in population and organisation, becoming village communities and proto-urban settlements, located near to each other in order to have a proportional consumption of agricultural resources. This suggested to archaeologists a widespread colonisation process started during the 9th century BC which led to four main Etruscan areas: a southern region, including the future cities of Veio, Cere, Tarquinia and Vulci; a central-northern section between two important rivers, Tiber and Arno; an area concerning the current Campania in the South, with a core around Capua; and a north-east region regarding the current Po Valley with the establishment of Felsina. Settlements raised in this period consisted in small oval huts made of clay walls built on foundation channels with a wooden supporting structure covered by a wooden roof.

Necropolis of Villanovan culture occurred as large fields of urns with burials placed into wells dug into the ground or into rocks. Biconical urns were decorated with meander, metope and lines patterns, with a lid that distinguished the gender: helmet-shape for male and bowl-shape for female. Nevertheless, in the southern territory of Etruria also a different type of burials was found: in addition to the biconical urns, hut-shapes urns were noticed suggesting a particular social role of the dead. These urns were used exclusively for a male person denoted as a warrior and a *paterfamilias*.

Some urns were accompanied by artefacts imported from production areas outside Italy, testifying contacts with other cultures. These objects could be considered as commercial exchanges and/or as

gifts between chiefs, or as personal belongings of foreign people well integrated into the Etruscan society.

In the 8th century BC the urban aspect experienced important changes; some establishments started to develop arriving to control other villages, that eventually disappeared. This scenario led to the rise of cities with relevant demographic and economic power, dominating all over the surrounded areas and taking local control of trade and agricultural production. Not all the city sites were completely built and populated, but some were used also for vegetable growing, agriculture and stock breeding. From the 7th century BC the process of urbanization increased, introducing the roofing technique which consisted in covering the roof structure with decorated tiles and terracotta. In this period the ceramic manufacture split into big containers production, tiles and tableware production.

In addition to the roof covering, some architectural modifications were noticed due to the observation of the aristocratic tombs. In the city of Cere, tombs were structure with the aim to resemble to the domestic house, which was not anymore characterized by the oval hut structure but was composed of rectangular perimeter, permanent masonry, stone skirting board and mud bricks wall. These radical changes were the consequences of the arrival of Phoenician and Greek traders which were attracted by mineral resources of Etruria and were the importers of different goods and ideas. As mentioned above, rectangular floor plan took the place of the oval one, stone foundations replaced sunken channels, mudbrick walls were preferred to wattle-and-daub, and roofs were covered with fired clay tile instead of straw.

It was during the 6th century BC that the process of urbanization was completed, introducing the distinction of political, religious, public and private areas. Po Valley started to be urbanized in this period, replacing the ancient Villanovan villages previously founded, affirming the significant presence of an Etruscan society, with the definitive development of Felsina and the creation of colonial cities such as Marzabotto, Mantova and Spina.

Before this colonization the Polesine area presented a different aspect. Between the III and II millennium BC it represented an important trade point of various commercial routes between Europe and the Mediterranean Sea. Settlements were situated close to the water courses, mainly in the surroundings of Tartaro river and "Po di Adria", which was the principal branch of the ancient Po and a convenient access to the Po plain. Evidences of Bronze Age in the northern Polesine were found in the surroundings of Tartaro River with the discovery of a stilt village at Castelnovo Bariano. Here the main human activities were agriculture and breeding, having close economic and cultural relationships with the populated areas of north Italy, but also of central and eastern Europe. Subsequently, the number of settlements grown rapidly, reaching a peak in the 13th century BC.

Villages were surrounded by a moat full of water and an earth embankment, with the function of defensive structure.

The diffusion of precious goods such as amber coming from the north and ivory from the south, coupled with the spread of the glass manufactory technology (coming from the Near East) led to a flourishing period for that region, which became a crossroads of trade routes and traders of different origin. Craft activities improved, such as amber and bone processing, glass production and metallurgy, increasing the wealth of centres like Frattesina, which become an international *emporium* between 12th and 10th century BC.

Polesine continued to develop, becoming the most important trade centre in the zone. It represented a trade interchange area, linking Adriatic Sea, Tyrrhenian Sea, Aegean Sea, Balkan Peninsula and Central Europe. Nevertheless, at the beginning of Iron Age these settlements were abandoned forever. In this scenario, the massive migration of Greek people took place, searching for new fertile lands.

1.1.1 San Basilio, Adria and Spina settlements

At the beginning of 6th century BC, the region between the Adige and Po rivers represented the border area between the Etruscan and the Veneti domains, being the core of an intense phenomenon of cultural interchange. During this period the area close to the Adriatic harbours became a crucial point for the exchange of ideas and mythical/religious traditions. In the Po delta landscape, San Basilio represented not only an important harbour, but also the place where different cultural and commercial entities met, as well as the bazaar of the Adriatic and Mediterranean world. This convergence between different populations is testified by several archaeological findings, especially the pottery. The domestic pottery was of local productions and of Venetic type, whereas the black and grey *bucchero* and the pink pottery with red or brown geometric decorations were imported from northern Etruria. Moreover, some Corinthian and Attic red- and black-figure cups, coming from eastern Mediterranean, were of great prestige because of their faraway origin.

Figure 2. Po Valley territory during the Etruscan period (Bonomi, et al., 2000).

Moving inland, the ancient settlement of Adria was settled between Adige River and the main course of the Po River, becoming a fertile territory for agriculture and farming. It grown in an unstable geomorphological context, needing particular building techniques; houses employed simple and

perishable construction materials, such as wood, earth and straw, while foundations were characterized by wood, soil and draining layers, reflecting the effort required by the wet unstable environment. Furthermore, between 6th and 5th century BC some buildings were both houses and craft laboratories. Adria became soon an important commercial port in the north Adriatic region, trading with Greek, Etruscan and Transalpine populations. Its harbour was the most northern on the Adriatic Sea and an extremely important centre for the maritime control: Etruscan and Greek goods were received here to be then delivered by river towards the hinterland and across the Alps. It represented a central connection point between the Sea and the inland, as well as a waterway of particular relevance; furthermore, the harbour, settled eastward, allowed contacts with the one in Spina. Adria became so important in those years, that it gave the name at the surrounding Sea.

Another significant settlement of the area was Spina, established along the mouth of a Ferrarese branch of the Po River and the Lake of Comacchio, becoming one of the main trade centres in the Delta Region. It was created as commercial outpost with the function of supervising the river mouth and its basin, as well as the large lowland area. In this occasion the regular grid of streets was replaced with a large number of navigable canals. The type of settlement and the necropolis, with tombs made of simple wooden boxes but luxurious grave goods, denoted a prosperous society of merchants and sailors. Despite the high degree of autonomy on the political level, Spina was strictly dependent on Felsina. This is testified by the finding of the grave stela[1] of Bologna, that represents an Etruscan boat with some warriors and oarsmen. The grave belonged to a member of an illustrious family of Felsina, probably a commander of a defensive fleet on the Adriatic Sea, reporting to Spina (Sassatelli, 1990). The city was considered as an *empórion*, inhabited by a population which included a large portion of Greeks and Veneti too. Spina was considered the core of the commercial network, where trades with the Greeks were far greater than in the Tyrrhenian side.

Nevertheless, after the culmination concerning the 5th century BC, this system started to collapse definitively with the Gallic invasions at the beginning of the 4th century BC. These attacks led to deep changes in the cultural and regional layout of the Po Valley territory, moreover the urban structure settled by Etruscan was set aside causing displacements and a demographic decline.

1.2 Etruscan building techniques

This section intends to help the comprehension of the different Etruscan building technologies and the typologies of materials used. The archaeological findings under investigation are supposed to be non-vascular ceramic materials used for covering house walls, however in this study the use for covering roof or floor is also taken into consideration.

---

[1] http://www.museibologna.it/archeologico/percorsi/47680/id/48046/oggetto/48055/

1.2.1 Wall building techniques

In archaeology the interpretation of walls is necessary to understand and describe domestic architecture, but it is well known that walls and roofs do not survive particularly well compared to foundations. Concerning the Etruscan period, a wide variety of wall building techniques can be found in the literature, but usually they are grouped into two main categories depending on the material used. One group is characterized by walls made of wattle or *pisé* and the other one by walls made of mud brick or stone (Miller, 2017). This classification is almost used to underline the architectural transition between the hut and the house, since the hut was a temporary structure made of wood, whereas the house was considered a solid structure of stones and bricks.

The main wall building methods for Etruscan domestic architecture are non-stone walling techniques and stone walling techniques. Moreover, a further distinction is made between structural and infilling systems.

Self-supporting system is considered one of the main different types of structure identified in non-stone walls. It is made of the same materials as its infill and it supports its own weight, as well as extra stresses coming from the rest of the building. As opposed of this latter, timber-framed structure is composed of wooden poles and beams that bear the brunt of the entire building, passing the weight pressure of the wall and the roof into the foundations. It is also possible to have a combination of both, called half-timber system, carrying load and stresses but having the timber frame separate from the walls.

The infill is a non-structural element designed to act as insulation and various forms of construction were employed to create infill walls, such as wattle, *pisé* and mud brick.

Wattle consists of a lightweight construction material made by blending thin wood slats between vertical stakes to form a woven grid of strips, in Italian called *incannucciato*. The technique goes back to Neolithic times, when it was figured as a technological innovation for the practice of house construction in Southeast Europe (Stevanović, 1997). It is often considered the most common infill used in early Etruscan walling, usually covered with daub, a sticky material mostly made of a combination of wet soil, clay, sand, animal dung and

Figure 3. Illustration of the half-timber walling system with the use of wattle as infill (Miller, 2017, p. 163).

straw, used both as a binding agent and as an insulator. Concerning timber framing the wattle may be place between the main structural poles of the wall and then covered in daub, otherwise it may be made *in situ* to form the whole of a fence or wall. The trace we had of the real existence of this

technique is found in the impressions left by the framework in fragments of daub. This is the case, for example, of a domestic structure belonging to the Etruscan settlement of Forcello di Bagnolo San Vito, in the municipality of Mantova. The habitation was dated back to 475-450 BC and several daub fragments were found suggesting the wattle and daub construction technology. Moreover, the presence of clay coating on quite a few numbers of *concotto*[2] demonstrates the practise of covering the daub wall with plaster, using a more liquid material suitable to be smoothed (Croce, et al., 2014). Another example of *incannucciato* findings came from the first housing unit concerning the city of Marzabotto, a well-established Etruscan colony near Bologna, dated back to the 5th century BC. From the analyses carried out in 1995 on clay fragments it was proved that these materials underwent a firing process; since then the common idea was that this kind of plasters were applied raw to the wattle (Minguzzi, et al., 1995).

Pisé is an ancient technique, traditionally defined as "rammed earth". The oldest evidence of this method has been found in Neolithic archaeological sites in China, but it was used for Etruscan domestic architecture in Italy as well. The construction of a complete wall begins with a temporary wooden frame, called "formwork", use as a mould to obtain the desired shape and dimensions. The earth is pressed downwards from
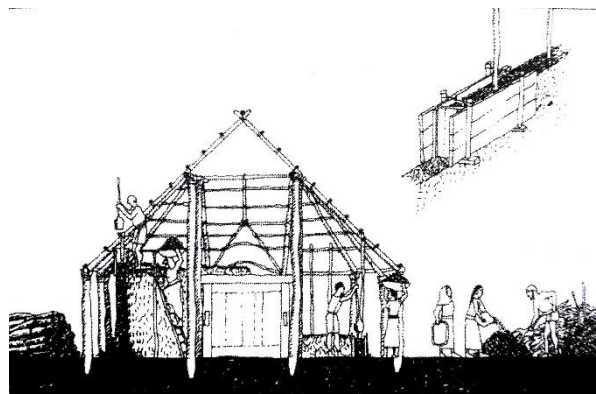
Figure 4. Illustration of a timber-framed structure with pisé walls (Miller, 2017, p. 155).

the top in different sections and time, until the formwork resulted fulfilled and compact. Subsequently the frame can be removed and use for a second part, in order to obtain the entire wall. It is left to dry in the sun, with the consequent decrease in volume, and finished with plaster or daub. *Pisé* structure differs from wattle in term of supporting stress, since it has the power to sustain its own stresses and also the rest of the superstructure, being defined as self-supporting. Furthermore, it is considered as an alternative use of wattle and as a probable sign of adoption of foreign (namely Greek) building concepts (Miller, 2017). Direct evidences of *pisé* walling are not so easy to detect. Fragments of clay found in and around the foundation of a structure could suggest the use of this wall system, even if the use of clay as the main component in a *pisé* wall would cause a structural failure.

The use and development of mud brick was considered as an evolutionary step in the Etruscan architecture, produced by the adoption of Greek customs and techniques. This technique may be seen

---

[2] It has been decided to maintain the Italian word *concotto* where present in literature, since Italian archaeologists adopt it referring to the mixture used to create construction and architectonical artefacts or unidentified non-vascular fragments (Tasca, 1998).

not only as a non-stone method, but also as representative of the changes in buildings perception; in the 7th century BC technology used in domestic structures varied as a consequence of the changing perceptions of space. Bricks were formed using a wooden mould filled with clay soil wet and mixed with organic inclusions and then left to dry. Successively, they were assembled together with a coating of daub or lime.

1.2.2   Roof and floor building techniques

In his research Miller (2017) proposed a sort of dataset for the interpretation of Etruscan architectural changes through time. He focused on central Etruscan settlements from the 8th to the 5th century BC subdividing different foundation techniques, called *Type 1, 2, 3, 4* and *5*. He asserted that the sequence that produces foundations was composed of four independent operations: ground preparation, wall footing, flooring and roof support.

He did not take into consideration archaeological site and findings from the Padan Etruria, but his study could be useful to understand roof and floor building techniques, since Etruscans from the central Etruria started to colonize the norther territory around the 6th century BC.

Frequently, there are no *in situ* roofs, but the identification of roofing techniques is possible through the available direct evidence.

Miller (2017) defined *Type 1* foundations set into bedrock with bedrock-cut channel wall footings, that held permanent structures reducing chances of soil deformation, rots and erosion. Concerning the roof, he specified that the elliptical buildings corresponded to a three-aisles type roof support, while the rectangular structures presented two-aisles or single-aisle support, covered by straw. *Type 2* differs in ground preparation and wall footing, showing a prepared soil and stone skirting boards. The floor layer is placed above a smoothed surface covered by one layer of clay, followed by a coating of cobblestones covered itself by an additional layer of clay. However, evidences of roof supports are absent. *Type 3* foundations present a semi-subterranean ground preparation technique and are set into bedrock or soil with no apparent wall footings. The floor is cut out of the ground, as a carved and pressed earth floor and even in this case no evident roof supports were found.

Miller (2017) designated *Type 4* and *5* in the Orientalising and early Archaic period (625-500 BC), referring to these buildings as houses instead of the previous huts. In fact, in the 7th century BC, the contact with other cultures has brought a radical change in the construction methods: the floor perimeter becomes rectangular instead of oval, stone foundations were introduced as well as fired clay tiles for the roofs (Winter, 2017).

Type 4 foundation was considered as an evolution of *Type 2* setting into a prepared soil, not on bedrock, and showing the same typology of wall footing. Despites the similarities, *Type 4* brings

some modernisation in the design of the domestic space, such as the creation of a multiple structure unit, as well as in the wall footings, building a stronger overall structure which can bear greater pressure, as suggested by the introduction of tile roofing system. *Type 5* foundations present feature of both previous Types: the foundation set upon a bedrock in order to create a level surface is an evidence of *Type 1* and *3*, whereas the creation of soil deposits is similar to *Types 2* and *4*. The ashlar stone skirting board could be seen as the innovation of *Type 2* wall footing. No evidences in foundations for roofs were detected, since the weight of the tiled roof was transferred to the ground by the walls (Miller, 2017).

1.3 Ceramic materials

This chapter provides an introduction on ceramic materials, focusing on the ceramic composition and on the firing procedure, in order to better understand chemical changes during the production process. Analysing the heating process, it is possible to estimate and evaluate firing conditions and technologies applied by the producer.

1.3.1 Compositional characteristic of ceramics

The main raw constituents forming the ceramic mixture are clay minerals, non-clay minerals, sand and water, necessary to create and model the paste.

Clays are the most important component of a ceramic body and represent a natural aggregate of clay minerals and accidental minerals. Clay minerals are phyllosilicates chemically composed of hydrate aluminum silicates. The basic structure is based on two main units: a six-member ring of $[SiO_4]^{-4}$ tetrahedra (T) and a sheet of octahedra (O) (Figure 5) linked together through oxygen.
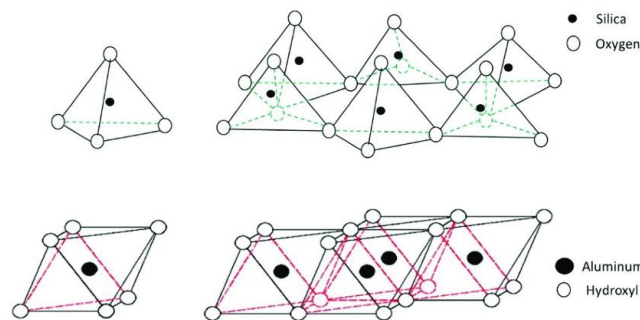
Figure 5. Tetrahedral and octahedral structures of phyllosilicates (Genedy, et al., 2014).

Clay minerals can be divided into 7 groups based on their crystal structure, however in this study only three of them are considered, since they are the principal minerals used for ceramic production (Cuomo di Caprio, 2007):

- Kaolinite group presents a lamellar structure of alternating layers T-O. The principal mineral of the group is the kaolinite ($Al_2Si_2O_5(OH)_4$), characterized by weak bonds between layers, giving poor hardness to the material. Furthermore, these bonds do not allow water to enter in the interlayer, causing hard workability and easy shredding.

- Micas group displays lamellar structure of alternating layers T-O-T with potassium cations (K^+) in the interlayer. Illite, represented by the formula $K_yAl_2(Si_{4-y}Al_y)O_{10}(OH)_2$ with y usually less than 2, is the main mineral used in ceramic production and entails good workability and plasticity.

- Smectite group presents a structure of T-O-T layers with cations (usually Ca^{2+} and Na^+) in the interlayer that can surrounded themselves with water molecules, forming interstitial water and causing swelling. Montmorillonite is the most important mineral of the group, showing excessive plasticity and difficult workability. The general formula is $(Na, Ca)_{0,3}(Al, Mg)_2Si_4O_{10}(OH)_2 \cdot _n(H_2O)$.

Non-clay minerals are already present in clay as natural components or are added deliberately by the producer as supplements with the purpose of modifying some characteristics, such as reducing the plasticity and decreasing the melting temperature of clay minerals. These materials are called "degreasing" and "fluxes".

The group of degreasing consists of other silicates, as quartz and feldspars. Quartz (SiO_2) is the principal silica mineral, being widely used thanks to its high stability under firing conditions. Feldspars are tetrahedra with atoms of silicon and aluminium in the centre, linked together through the four oxygen corners, creating a sort of cage. This family is known under the name of tectosilicates and the main components are K-feldspars ($KAlSi_3O_8$), albite ($NaAlSi_3O_8$) and anorthite ($CaAlSi_3O_8$). The main component in the group of fluxes are carbonates and oxides. Carbonates are calcium carbonates in the form of calcite ($CaCO_3$) or dolomite ($CaMg(CO_3)_2$), while oxides/hydroxides are mostly iron oxides/hydroxides as hematite (Fe_2O_3), goethite ($FeOOH$) and limonite ($FeO(OH)_n \cdot H_2O$), which are responsible of the coloration of the final ceramics.

An additional group can be identified as accidental materials, that are composed of organic compounds, fossils, heterogeneous materials, etc. They could be naturally found in sedimentary rocks, intentionally added from producers or accidentally present in sands.

1.3.2 Chemical reactions during firing procedures

Particular regard is given to the firing process, since it is the phase during which chemical and physical reactions occurred on ceramic components in order to obtain a hard and durable object.

The traditional firing method can be promoted choosing between two main systems: kiln firings, involving permanent structure with a firebox, and open firings, considered as every other type of structures that require the direct contact through fuels and artefacts.

Firing atmosphere influences the final coloration of the ceramic, according to the high or low presence of oxygen. In addition, oxidizing atmosphere promotes a light coloration since carbon originated from the fuel is consumed, while in reducing atmosphere carbon deposits on the ceramic surface leading to a dark brown colour.

Hereafter the attention is focused on chemical and mineralogical changes occurring in the clay matrix. A first range of temperatures can be attributed from room temperature until 200°C, in which water absorbed in the material, as well as interstitial water, evaporates without any structural changes.

The subsequent range covers a wider domain, from 200°C to 700°C. The most important irreversible reactions occur in this step. Between 300°C and 600°C the organic materials decompose; CO_2 and steam are produced during this phenomenon when it happens in presence of oxygen, meanwhile in loss of oxygen the atmosphere is reducing, and the carbon particles can react as reducing agents with iron oxides, potentially leading to the formation of magnetite as follows (Campanella, et al., 2007):

$$Fe_2O_3 + C \rightarrow 2FeO + CO$$

$$FeO + C \rightarrow Fe + CO$$

$$4FeO \rightarrow Fe_3O_4 + Fe$$
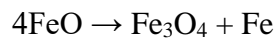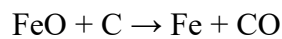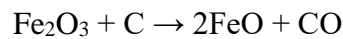
Furthermore, magnetite can be produced from the reaction of carbon particles directly on hematite through the following reaction (Campanella, et al., 2007) :

$$2Fe_2O_3 + 2C \rightarrow Fe_3O_4 + 2\ CO + Fe$$

Hematite forms at low temperature with the dehydroxylation of goethite (Campanella, et al., 2007):

$$2FeOOH \rightarrow Fe_2O_3 + H_2O$$
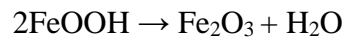
Above 450°C the elimination of chemically bond water in clay minerals occurs, even if every mineral has its own specific range of temperatures. Hydroxyls need high thermal energy to be removed, leading to the collapse of the crystalline structure which cannot return to the initial state (irreversible reaction). Kaolinite undergoes dehydroxylation around 650°C transforming into metakaolinite:

$$Al_4[Si_4O_{10}](OH)_8 \rightarrow 2Al_2Si_2O_7 + 4\ H_2O$$
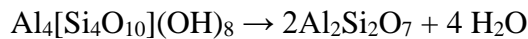
This process is accompanied by a mass loss of approximately 14 mass % (Zemenova, et al., 2014) and is characterised also by an endothermic reaction. Montmorillonite dehydroxylates around 500-550°C, when a proton moves from one hydroxyl to an adjacent one forming a water molecule and Al^{+2} coordinate with the remaining oxygen (Stevenson & Gurnick, 2016). The presence of cations of the illite interlayer inhibits the intrusion of water; the structure endures until the initial beak down between 700°C and 850°C, that leads to the total collapse at 1100°C (Stevenson & Gurnick, 2016).

Quartz is defined an inert mineral due to its chemical stability, since it does not react with other components during the firing process until 1000°C. It presents polymorphs depending on the temperature: α-quartz until 573°C, β-quartz until 870°C, trydimite until 1470°C and after this range

cristobalite until the melting point at 1710°C (Cuomo di Caprio, 2007). It must be considered that these transformations are reversible, consequently during cooling process β-quartz could return into α-quartz structure with a contraction in volume equal to the expansion occurred during heating.

Above 700°C the carbonates dissociation takes place with the decomposition of calcite into calcium oxide, releasing CO_2. This reaction is completed around 870°C according to the following reaction (Cuomo di Caprio, 2007):

$$CaCO_3 \rightarrow CaO + CO_2\uparrow$$
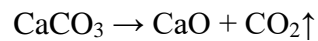
At 900÷1100°C the crystalline lattice of clay minerals is completely destroyed, and new high-temperature phases are formed, such as wollastonite ($CaSiO_3$), gehlenite ($Ca_2Al_2SiO_7$), diposide ($CaMgSi_2O_6$) and anorthite ($CaAl_2Si_2O_8$) (Ravisankar, et al., 2010). Moreover, vitrification processes and glass formation usually begin at around 1100°C, driving to physical alteration as shrinkage due to the development of close porosity.

1.4 Case Studies

In this study selected ceramic samples from two different archaeological sites have been considered: San Basilio and Adria. The sites were both located in the Po Valley, precisely in the county of Rovigo. Since excavations were conducted in different times (1983 and 2016), the archaeological approaches were dissimilar and consequently also the information written on the reports. Hereafter are reported almost all the material released.

In addition, a third site has been considered as a reference, because the ceramic materials found presented same morphological features compared to those under investigation.

1.4.1 Archaeological site of San Basilio (RO)

Nowadays San Basilio is situated 20 kilometres far from the sea, belonging to the city of Ariano nel Polesine located in Veneto. The area is situated between Venezia Po (north) and Goro Po (south) and it is known as Ariano island.

During the 80s, some evidences of a pre-Roman settlement were found as a result of agricultural and smoothing works, therefore in 1983 an excavation probe was carried out. The Archaic settlement was based on the western edge of a seaside dune belonging to the complex system of fossil duny cordon that crossed the whole Delta area from north to south. S. Basilio cordon, known as "*cordone II*", represented a beach line well established in the 6th century BC, at the same time as the formation of Adria. The ceramic fragments found during the digging allow to date this sector of the site back to the second half of the 6th century BC and the first half of the 5th century BC. They also give evidence

about the coexistence of local and Greek people and confirm the cultural and trade relation with the Etruscan population settled in the Emilian area.

Three anthropic layers were identified in the excavation survey, revealing that the settlement was characterised by two distinct phases, even if directly subsequent. Stratigraphic units are not indicated, however findings were subdivided according to the stratum.

Clear evidences of housing structures were found in the top layer: remains of paving made of clay hardened by fire, charred pieces of poles and fragments of plaster made of clay with reeds and branches prints. It was deduced that clay, timber and twig were the main building materials, since stone structures would be too heavy for a marshy ground. Moreover, clay fireplaces and ceramic artefacts for domestic use were detected within the perimeter of the human habitat: black- and red-figure Attic pottery with floral decoration, some fragments of Corinthian ceramic and some of black- and red-band Paleoveneta ceramic, lots of *bucchero* fragments and common Etruscan ceramic. Moreover, clay materials waste indicated that the settlement was well organized for domestic production of pottery.

The second stratum was identified as a soil with the function of raising the layer below; this latter was full of *bucchero* fragments, domestic animals' bones and wooden structures, such as vertical poles and horizontal planks, suggesting a more residential purpose.

Therefore, the lower layer corresponded to the older phase in which the settlement was designated to *bucchero* processing or storage. When these structures became obsolescent, probably due to flooding, the area was completely reclaimed and filled with soil over. The level above was the most recent archaeological stratum, representing the youngest phase designed as residential use .

Since the whole area is not completely explored, the real extension of the settlement is not yet known[3].

1.4.2   Archaeological site of Adria (RO)

Nowadays Adria is situated 25km far from the Adriatic Sea, in an area outlined between Adige River in the north and Po di Goro in the south.

Evidences of a residential nucleus were detected already in 2004, however it was not until the spring of 2016 that it was accurately studied.

During 2015 and 2016 an excavation was carried out in the nearby of the city centre, bringing out archaeological settlements from different periods. The work was divided in three distinct tranches: the first corresponding to the Late Roman-Early Medieval period, tranche II referring to the Hellenistic period and the third one to the Greek-Etruscan ages. This latter was an open area

---

[3] Some archaeological excavations were carried out in the summer-autumn 2019 from the Archaeological Department of Ca' Foscari University of Venice, and the University of Padua.

excavation of the western area concerning the previously uncovered tranche II. It referred to the wooden frame building on platform excavation dated to the 6th and 5th century BC, and it was divided into ten different phases as follows:

- phases 1A and 1B, including pre-platforms strata and the position of the so-called "*fossato umido*";
- phase 2, including the platform preparation, the footing system with beams and plinths, and the perimetral wooden frame regarding compartments of structure A and B;
- phase 3A and 3B, concerning the residential frequentation of structure A (rooms 1 and 2) and B (north and south sectors), with evidences of fireplace in room 2;
- phase 4A and 4B, regarding partial walls collapses and flooding, followed by a structural removal due to a temporary abandonment of the area, and evidences of fire on beam;
- phase 5, revealing a re-frequentation of the area with implant of squared plinths and platforms with discarded ceramic tiles fragments;
- phase 6, indicating the first phase about the big flooding;
- phase 7, including the excavation of the so-called "*fossato asciutto*" and evidences of the ditch used for the toasting of grains;
- phase 8, indicating a second flooding;
- phase 9, revealing wells for the melting of small bronze artefacts and a floor full of ceramic fragments;
- phase 10, concerning flooding.

Since the archaeological report is highly detailed, hereafter are reported only the stratigraphic units (SU) in which non-vascular ceramic fragments were found.

Phase 2 could give some information about the building technique since some wood plinths were distinguished in compartments 1 and 2 of structure A, upon which some perimetric wood beams were placed originally defining the space. Furthermore, Structure B also presented ligneous structure with a support function for the overlaying beams, identified as the bases of the wall timber frames. These latter are connected with the ground through vertical poles or blocks positioned near intersections or carved into the plinths.

Phase 3 revealed a pit filling with discarded archaeological materials entitled SU 4098, that appeared to be subsequent to the abandonment of the area. Moreover, a stratum of branches, twigs, *graticcio*[4] and beams denoted a collapse of the wall wooden frame, suggesting the use of wattle as a filler in the building technique. This layer was covered by a sandy depositional stratum, SU 4095, with some non-

---

[4] The Italian word *graticcio* had frequently caused misunderstanding in English archaeological terminology, being translated as wattle and half-timbering without distinction. The choice was to maintain the Italian word as written in the archaeological report, preventing incorrect translation.

vascular ceramic fragments. In room 2 of structure A, a fireplace was found with a hardened slab of clay loam that appeared to be connected with SU 4096, that unveiled chunks of charcoal, remains of ashes and pieces of *concotto*. This room was identified as an area for metallurgic works.

Woods structural elements regarding structure B were found in phase 4, as remains of windows frames, wall pieces of *graticcio* and beams without evidences of air or sunlight exposures. This led the archaeologists to advance the theory of a structural removal prior to flooding; since no roof remains, as well as domestic ceramics, were found, some useful elements could be removed in order to be used in other places or for different functions.

After the abandonment phase, compartments 1 and 2 displayed sediments accumulated during the flooding phenomenon. Phase 5 revealed platforms with discarded ceramic fragments in structure A, SU 4063-4065 that covered SU 4095. These strata were sealed by a flooding depositional layer, SU 3268, concerning phase 6.

In SU 4106 were found fragments of discarded ceramic tiles, laying on the west edge of a ditch oriented east-west. The latest layer to display *concotto* fragments was SU 3264 in phase 10, sealed by flooding deposition.

1.4.3   Archaeological site of Spina (FE)

Spina Adriatic harbour was founded during the second half of the 6th century BC near a branch of the Po Delta in Emilia-Romagna. The settlement conditions were advantageous due to the proximity to two more river courses.

Some excavation works began around 1920, but it was at the end of the 50s that something took the attention of the archaeologists: aerial photos revealed the possible localization of a settlement. Some evidence was noticed due to a natural fact, the drainage of the eastern valley. However, the area started to be examined only when it was completely drained, in 1964. In subsequent years (until 1981) different excavation campaigns were conducted and several findings were then collected, such as ceramic artefacts, amphorae and structural elements.

The oldest phase consisted of a portion of a residential building, dated back to the last quarter of the 6th century BC. The structure, called Structure 1, was partially conserved thanks to the surrounding anaerobic environment and to the fire that probably hit the house. The presence of fired clay, with branches prints on it, suggested two possible construction techniques: walls could be composed of overlapped plastered timbers, as in alpine wooden houses, or could be created with a mixed technique using raw clay.

A significant layer of clay covered the older phase, probably as a consequence of grading works or a natural flood. This was a slightly recent phase than the previous one, around the last decades of the

same century. Stuck into the ground were two parallel rows of vertical wooden poles, fourteen in total, no more than a meter tall. They seemed to uphold few horizontal wooden planks with the function of plinths, above which laid a huge amount of *concotto*, *incannucciato* and plaster fragments, whit even charcoal and ashes. All materials belonged to the so-called Structure 2.

Proceeding with the strata, Structure 3A and B were intended as domestic buildings due to the presence of some fireplaces. Lots of *incannucciato* and plasters pieces were found also here. Findings from 3A were dated between the end of the 6th century BC and the beginning of the 5th, while the ones from 3B indicated a younger phase corresponding to the half of the century. This latter was thought also as a loading area, considering the presence of a distinct area full of pantry ceramic items, *incannucciato* and plasters.

In the surrounding area, a section of a canal was discovered, pointed east-west. It was filled with thousands of ceramic fragments covering a period of 100 years, from the mid- 5th century BC to the mid- 4th century BC. Structure 5 was detected right on top of the canal, and it could be from the same period. Human activity was detected by means of the identification of fireplaces, pantry ceramic fragments, loom weights and a spatula made of bone.

In the western sector, Structure 6A and 6B were separated by 20 cm of clay and were dated back respectively to the first quarter of the 5th century BC and the half of the century, both reflecting the assumption of a fire collapse. Around one thousand of *incannucciato* fragments were collected in both structures, whereas little more than 1500 pieces of plasters, called *mattonato*, were found exclusively referring to the Structure 6A. Moreover, the discovery of loom weights testified the domestic inhabitants' activities.

Considering the building techniques, evidence from Structure I testified the use of the *Blockbau* technique. It was a system widely used since the Neolithic Age in Central Europe; the approach was to create a self-supporting and self-locking perimeter composed of horizontal wooden beams embedded with others at the edges (Zamboni, 2016, p. 54). Related to the constant presence of huge amounts of *incannucciato* and plaster pieces, the wattle and daub methods was suggested for the creation of walls.

2. MATERIALS AND METHODS

The chapter focuses on materials and methods employed for their characterization. The first part describes the domestic ceramic fragments found in the archaeological sites of San Basilio di Ariano Polesine and Adria, dividing them into groups according to macroscopic features.

Furthermore, a summary of the diagnostic methods followed is given with the description of set-ups and the explanation of what kind of information these techniques provide for ceramic materials. A multi-analytical approach was applied in order to investigate chemical composition, mineral phases and firing conditions of non-vascular ceramics.

2.1 Samples description

Non-vascular ceramic samples, stored in the depository of the Museo Archeologico Nazionale di Adria (RO), have been considered in this study. 248 elements come from the 1983 San Basilio (SB83) excavation and other 201 represent the archaeological site of Adria, taken in 2016 (AER16).

Figure 6. General overview of non-vascular ceramic samples (SB83 and AER16). Depository of the Museo Archeologico Nazionale di Adria (RO).

They have been classified as fragments since they appear to be parts of a larger whole broken off, and few of them could be assembled back together (Figure 7 and Figure 8). They are different in size and shape, with a surface that goes approximately from 10 cm^2 to 110 cm^2 and a non-uniform thickness around 1.5 cm.

Figure 7. Samples 1-4Y_SB83 connections.

Figure 8. Samples 322-323W_AER16 connection (side A and B).

They manifest two dissimilar sides: one seems to be smoothed (from now on called side A), the other side (called B) is rough and irregular, in some case also flaked. A substantial portion of fragments has, on side A, a repetitive groove which differs between the sites; 70 pieces from SB83 show a deep and tight sign, whereas, 109 findings from AER16 feature a large, flat and shallow groove (Figg. 9-10).

Figure 9. Sample 3W_SB83. Deep and tight groove.

Figure 10. Sample 328W_AER16. Large and flat groove.

All objects present similar morphology, and some display particular details such as fingerprints impression on one edge and a sort of twisted decoration on surface A, as shown in Figure 11 and Figure 12. These are clear evidences of the hand-crafted realisation methods adopted by Etruscans; the attribution as decoration elements for the twisted pieces is just a hypothesis, since no other explanations seem to be suitable. Thirty-three fragments present fingerprints only on one edge and not on surface A or B, but the function of this pattern is not clear yet. It seems not to be a structural detail since no connection between the 33 different pieces was found, so it could be a sort of decoration for the final edge of a slab or a functional aspect in order to better paste with another material.

Figure 11. Sample 102Y_SB83. Twisted decoration.

Figure 12. Sample 1Y_SB83. Fingerprints impression.

Firstly, fragments were subdivided into groups depending on chromatic features, that could indicate differentiations in firing temperature and/or in mineral composition. The attention was focused on the pieces with one or more groove on surface A, dividing them into three main groups for SB83 and six groups for AER16, as shown in Table 1.

A particular evidence is that ceramics from Group A and 4 seem to be overcooked, going from a greyish to a violaceous colour, with some shades of white. Shreds from group 6 have some irregular patterns on the surface, like some crystal efflorescence. Most of the other fragments are red, pink and light brown.

Table 1. Groups subdivision of SB83 and AER16 concotto samples.

Site	Groups	Pieces	Colour[5]
SB83	A	14	Too much heterogeneous
SB83	C1	18	Light red (2.5YR 6/6)
SB83	C2	31	Light brown (7.5YR 6/4)
AER16	1	16	Light red (2.5YR 6/6) and reddish yellow (5YR 6/6)
AER16	2	14	Light reddish brown (2.5YR 6/4) with tones of pale yellow (2.5Y 8/2)
AER16	3	20	Pink (7.5YR 7/4) and very pale brown (10YR 7/3)
AER16	4	19	Light brownish grey (10YR 6/2) with some tones of light grey (2.5Y 7/1)
AER16	5	22	Red (2.5YR 5/6) with some tones of light reddish brown (2.5YR 6/4)
AER16	6	12	Too much heterogeneous.

Figure 13. 41W_SB83 group A
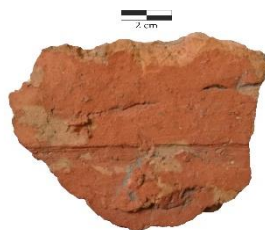
Figure 14. 2P_SB83 group C1

Figure 15. 20Y_SB83 group C2

---

[5] Based on Munsell soil color charts (Munsell, 2000).

Figure 16. Sample 302Y_AER16 group 1

Figure 17. Sample 303BL_AER16 group 2

Figure 18. Sample 313OR_AER16 group 3

Figure 19. Sample 318Y_AER16 group 4
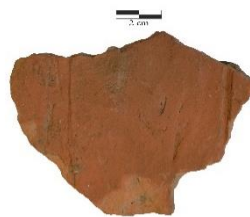
Figure 20. Sample 303Y_AER16 group 5

Figure 21. Sample 361BL_AER16 group 6

Moreover, few pieces from SB83 present variation in composition and morphology creating three more groups. Fragments from Group D show only one smoothed reddish surface without any groove on it, a greyish matte matrix with lots of small reddish inclusions and a width of 2.5 cm (Figure 22). Dissimilarly, shreds from group F present some angular structure that lead the hypothesis they were part of storage silos, with a whitish rough surface on the outside, and a reddish colour on the inside and along the section (Figure 23). Moreover, an additional group was made by the so-called decorations.

Table 2. Additional groups from SB83 findings.

Site	Groups	Pieces	Macroscopic description
SB83	D	11	Grey matt matrix with small red inclusion. One reddish surface.
SB83	F	10	3 big angular pieces. White rough external surface and red inner surface.
SB83	G	16	Decorations

Figure 22. Sample 6R_SB83_group D

Figure 23. Sample 13WR_SB83_group F

Furthermore, concerning SB83 findings, 210 fragments of *incannucciato* were also found stored together with the ceramic shreds. These pieces seem to present a sandy composition, since they display powdering to the touch. As it can be seen in Figure 24, these elements show circular longitudinal impressions on some sides, which are supposed to be fingerprints of the wattle frame, used for walling building technique.

Figure 24. Incannucciato samples: 1_INC, 2_INC

2.2 Investigation methods

A multi-analytical approach was applied in order to detect similarities and differences about the composition of ceramic mixtures and possible coatings, as well as to clarify the methodology of firing technique.

Considering the high number of samples stored in the depository of the museum, a micro-destructive *in-situ* investigation strategy was primarily chosen in order to select the most representative fragments. Subsequently, they were taken to the laboratory based on the Department of

Environmental Sciences, Informatics and Statistics of Ca' Foscari University of Venice, for further investigations.

2.2.1 Optical Microscopy (OM)

Light observations of selected samples were performed by two different instruments: Dino-Lite AM4113 digital microscope and Olympus SZX16 stereoscopic microscope.

Dino-Lite was used to observe sample surfaces in order to recognize similarities or discrepancies. Images were acquired through Dino Capture 2.0 software with a magnification of 50x.

Observations with the stereomicroscope were done on polished cross-sections obtained by embedding fragments of the samples in polyester resin and subsequently polished with decreasing grit abrasive papers. Pictures were taken using Olympus Camedia C-5050 camera at different magnification (7x, 20x and 40x) allowing to obtain information about the ceramic body in order to examine its main features.

2.2.2 Water absorption by total immersion

Procedure guidelines for establishing water absorption by total immersion are detailed in NORMAL 7/81. Results were determined by the change in mass of the sample after different periods of time of complete immersion in water. This technique gives indications about the absorption rate allowing the comparison of the open porosity between ceramic samples.

2.2.3 Fourier-Transform Infrared spectroscopy (FT-IR) and FTIR in Attenuated Total Reflection (ATR) mode

FT-IR spectroscopy is an investigation technique that allows the identification of the compounds present in the samples, used, in this study, for the chemical characterization of ceramic fragments. ATR is technique used in combination with infrared spectroscopy in order to analyse the chemical composition of samples in terms of molecular species. It was chosen as a preliminary *in-situ* analysis for the initial evaluation of samples composition, since it represents a non-invasive technique.

The infrared spectroscopy analyses were carried out with a portable Bruker ALPHA spectrometer equipped with ATR modulus based on a single-bounce diamond ATR crystal. The obtained spectra were the average of 32 scans acquired in the spectral range $4000 \div 400$ cm^{-1}. Sample were placed on the crystal head and were directly examined without any preparation.

Successfully, FT-IR was performed on selected samples in order to detect more punctual information about surfaces and bulk composition. Few mg of sample were finely pulverized with KBr powder and then pressed, in order to form a pellet that is then analysed.

The infrared spectroscopy analyses were carried out with Nicolet Nexus 670/870 FT-IR spectrometer. The obtained spectra were the average of 36 scans acquired in the spectral range $4000 \div 400$ cm^{-1} at a resolution of 4 cm^{-1} using KBr pellet technique.

The obtained spectra indicate the vibrational frequencies characteristic of the compounds in the samples, providing a fingerprint by which molecules can be identified. Elaboration (baseline correction, evaluation of the peaks, comparison with databases) was carried out with Opus (version 8.2.28) and Omnic (version 9) softwares. Spectra were also compared with data reported in literature, in order to assign the vibration frequencies to mineral families.

2.2.4 Thermogravimetry and Differential Scanning Calorimetry (TG-DSC)

TG-DSC is a method of thermal analysis in which the mass of a sample is measured while the temperature is changed over time, providing information about mineral phase transitions. In this study it allows the evaluation of the firing temperature of samples.

A differential scanning calorimetry was applied to determine the enthalpies; DSC curves allow the detection of exo- and endothermic peaks, caused by gain or loss of enthalpy occurring in the sample when undergoing controlled heating and compared to an inert reference material.

TG and DSC analyses were carried out simultaneously with Netzsch 409/C instrument. About 10 mg of finely powdered samples were heated in an open corundum (Al_2O_3) crucible from 25°C to 1000°C at a heating rate of 10°C min^{-1} with flow rate of 80 ml min^{-1} N_2. Data were collected and elaborated with TA Netzsch software.

Only few representative samples were considered for this analysis and the obtained thermograms were compared with data reported in literature.

3 RESULTS AND DISCUSSION

This chapter presents the results obtained from the analyses performed on the *concotto* samples from both archaeological sites, San Basilio and Adria, with the use of the investigation methods previously described.

The attention has been focused on the characterization of the analysed materials and their production techniques, in order to identify the main components and to better understand the firing conditions.

3.1 OM analyses

OM analyses allowed to better understand the macroscopic evaluation done by naked eyes. Tables 3÷14 show Dino-Lite images (50x) regarding surface A, B and sections of some selected sample in order to find similarities between groups, both SB83 and AER16.

As can be notice in Table 3, group A presents evident sings of heterogeneity on both sides and sections. Sides A display some dark spots and a general greyish coloration, whereas side B and sections appear to be light brownish in colour with some greyish spots.

Table 3. SB83, group A: Dino-Lite images, 50x.

	Side A	Side B	Section
41W			
44W			
102P			

Sides A of group C1 (Table 4) appear to be homogeneously red without any evident particular characteristics, while both sides B and sections seem to be light reddish brown.

Table 4. SB83, group C1: Dino-Lite images, 50x.

	Side A	Side B	Section
2P			
3P			
5OR			

No singular features have been detected also for group C2 (Table 5), showing a light brownish surface for both sides and sections.

Table 5. SB83, group C2: Dino-Lite images, 50x.

	Side A	Side B	Section
3R			
3W			
20Y			

Samples from group D (Table 6) show a greyish matte matrix with some reddish inclusions, as can be notice on side B and sections, and a reddish side A.

Table 6. SB83, group D: Dino-Lite images, 50x.

	Side A	Side B	Section
6GR			
6R			
8WR			

Group F (Table 7) presents two different sides, named as external (EXT) and internal (INT) referring to the possible outside and inside surfaces of the samples, that have been supposed to be part of silos. These two sides appear light greyish, while the sections light brownish.

Table 7. SB83, group F: Dino-Lite images, 50x.

	EXT	INT	Section
13WR			
14WR			

Table 8 represents samples from Group G, the so-called decorations. Considering the morphology, they were supposed to be placed on some kind of support showing the twisted part externally. Consequently, in Table 8 the name "Base" refers to the surface that should be in contact with the support, and "Dec" refers to the external twisted part. Bases appear to have a greyish colouration,

even if sample 106P presents some small reddish inclusion in the matrix. Meanwhile, Dec sides present different colour, reddish for 106P and greyish for 1BR, as for the base.

Table 8. SB83, group G: Dino-lite images, 50x.

	Base	Dec
1BR		
106P		
5V		

Samples from group 1 (Table 9) present reddish surface A similar to that of group C1, while side B and section show homogeneity in colour (light reddish brown).

Table 9. AER16, group 1: Dino-Lite images, 50x.
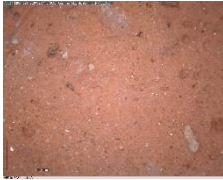
	Side A	Side B	Section
302Y			
306OR			
309P			

28
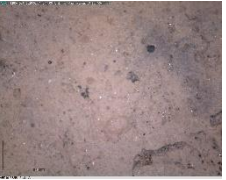
Table 10 displays images from group 2, showing a light brownish colour for all the surfaces, likewise group C2. Sample 305P presents a heterogeneous Side B, appearing more like group A.

Table 10. AER16, group 2: DIno-Lite images, 50x.

	Side A	Side B	Section
303BL			
305P			
339BL			

Colour of samples from group 3 (Table 11) seems to be similar compared to groups 2 and C2, even if appearing lighter (pale brownish).

Table 11. AER16, group 3: Dino-Lite images, 50x.

	Side A	Side B	Section
302W			
332BL			
362BL			

Samples from group 4 (Table 12) display a light grey side A, with some dark spots as for group A, but a more homogeneous light brown side B and section.

Table 12. AER16, group 4: Dino-Lite images, 50x.

	Side A	Side B	Section
304P			
309BL			
328W			

Group 5 (Table 13) presents a reddish side A and a lighter brownish side B and section, similarly to groups 1 and C1.

Table 13. AER16, group 5: Dino-Lite images, 50x.

	Side A	Side B	Section
303Y			
306Y			
341BL			

Sample form group 6 (Table 14) show a unique detail: all the surfaces seem to be cover by some crystalline efflorescence, that could be a depositional consequence concerning only the superficial area of the sample or some kind of efflorescence coming from the ceramic body.

Table 14. AER16, group 6: Dino-Lite images, 50x.
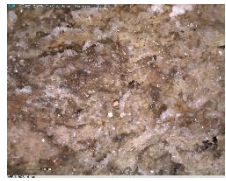
	Side A	Side B	Section
312Y			
361BL			
367BL			

Table 15 displays Dino-Lite images with a magnification of 225x in order to confirm the presence of crystalline efflorescence.

Table 15. AER16, group 6: Dino-Lite images, 225x.

	Side A	Side B	Section
312Y			
361BL			
367BL			

Finally, Table 16 shows *incannucciato* samples images (50x), displaying a different matrix considering *concotto* samples.

Table 16. SB83, incannucciato sample: Dino-Lite images, 50x.

1_INC	2_INC	3_INC
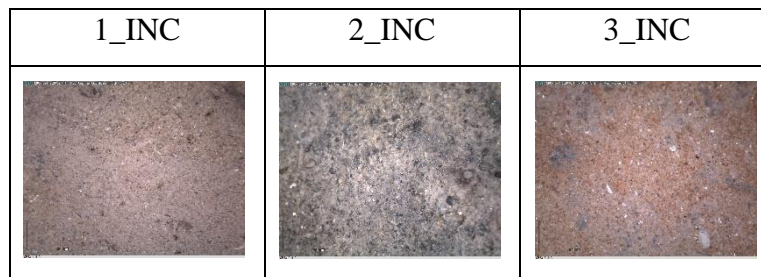
As a preliminary analysis, microscopic observations allowed to draw some general considerations:

- superficial evaluations seemed to validate the initial subdivision done by naked eye for samples concerning SB83 site;

- colour observations allowed to find similarities between some groups from AER16 site, consequently groups 1 and 5 can be arrange together, as for groups 2 and 3;

- groups A and 4 presented heterogeneity and some dark spots on both sides and sections, suggesting that something different should be happened compared to other fragments. It could have been a depositional factor or a consequence of different firing temperature;

- concerning group G (decorations), it was noticed that sample 106P presents similarities with group D, since both have red inclusions into a greyish matrix, sample 1BR displays a homogeneous pale brownish colouration as for group C2 and sample 5V resembles to group C1;

- group 6 was the only one displaying a particular aspect. According to the archaeological classification of the findings, these samples came from the same stratigraphic units; 8 fragments from SU 4106 and 3 from SU 4098. This could suggest a depositional formation of the efflorescence caused by environmental condition more than a compositional characteristic;

- moreover, some similarities between SB83 and AER16 groups were detected, such as between C1, 1 and 5, C2, 2 and 3, and also A and 4;

- *incannucciato* samples display a less compact matrix that seems to be composed of little grains.

Based on these considerations, observations with the stereomicroscope were done on polished cross-sections of selected samples, collecting information about the ceramic matrix and presence or absence of inclusions and cover layer. Few fragments were chosen depending on their features, with the purpose of underlying differences between ceramic bodies.

Table 17 shows stereoscopic images at different magnifications.

Table 17. Stereoscopic images. Magnification 7x, 20x, 40x.

Sample	7x	20x	40x
309P_1			
328BL_6			
41W_A			
6GR_D			
14WR_F			

Differences in colour and cover layer can be noticed between 309P_1 and 328BL_6; this latter presented a brownish colouration and a thin darker layer, that could refer to the superficial depositional stratum observed with Dino-Lite analysis. Three different layers were detected in sample 41W_A, probably related to different composition or firing conditions. A reddish layer was noticed also in sample 6GR_D, which presented some dark spots in the ceramic body.

As already observed by naked eye, sample 14WR_F displayed a greyish cover layer, suggesting an intentional coating applied by the producer.

In addition, some consideration can be done also concerning the visible pores: sample 328BL_6 seemed to be characterized by bigger pores compared to 309P_1, while the others displayed a more compact matrix.

3.2 Water absorption by total immersion

Water absorption by total immersion was adopted to investigate the porosity of the ceramic samples, revealing the quantity of water absorbed by the material submerged into water at room temperature and pression. This value is expressed as a percentage compared to the dry mass of samples. At least two representative samples for each group were considered. It must be recalled that, according to Dino-Lite observations, groups 1 and 5 have to be considered as a single group (from now on called 1+5), as well as groups 2 and 3 (2+3).

According to the NORMAL 7/81 samples should have the same shape and width, to directly correlate obtained values with the volume, and should be dried in an oven at 60°C before being weighed. For this study a different approach has been chosen, considering that a non-destructive strategy was recommended.

After being arranged in an indoor dry environment for weeks, selected ceramics were firstly weighed to register the initial value. Successively, they were submerged in a tank full of room temperature water and positioned above some holders in order to minimize the bearing surface. They were then weighed again after some specific periods of times until they reached saturation: 5, 15, 30, 45, 60, 90, 120, 180, 240, 300, 360 and 420 minutes. The time required to achieve sample saturation determines the water absorption behaviour of the ceramic fragments over time. Sample 1_INC was the faster to reach saturation (30 minutes), while the majority of samples (12) required 120 minutes, 5 fragments needed 150 minutes, only one piece required 240 minutes and two samples even took 420 minutes.

The quantity of water absorbed (WA) was estimated through the following equation (Normal, 7/81):

$$WA \% = \frac{M_t - M_i}{M_i} \cdot 100$$

where M_t corresponds to the mass at a certain time t, and M_i to the initial mass of the dry sample.

Table 18 shows the percentage value of each sample.

Table 18. Water absorption values.

Group	Sample	WA %
G	106P	14.53
3	302W	14.67
5	303Y	14.81
1	302Y	14.82
C2	3R	16.73
D	8WR	17.36
1	309P	17.58
C2	3W	17.60
G	1BR	17.69
A	102P	18.79
2	307P	19.04
C1	5OR	19.20
D	6GR	19.47
4	328W	19.54
4	309BL	19.96
2	303BL	20.22
F	26OR	20.25
F	14WR	20.96
A	44W	21.05
C1	2P	21.96
	1_INC	31.28

These values could be discriminants to understand which ceramic fragments reached similar saturation level. Since WA increases according to open porosity (Kato, et al., 2008), and high WA values are due to coarse particles (Velraj, et al., 2012), some considerations can be expressed:

- samples 106P_G, 302W_3, 303Y_5 and 302Y_1 presents the lowest WA value at around 14.71%, suggesting a composition of fine particles;

- most of the fragments analysed display similar values, ranging from 16.73% to 21.96 %. Additional subgroups are not so easy to identify because the numerical difference between one value and the subsequent is minimal;

- sample 1_INC shows the highest value of WA, suggesting higher open porosity and the presence of coarse particles.

The absorption curves are reported in Figg. 25-27, divided into three main classes depending on the absorption trends. As can be noticed, in Trend 1 the water absorbed in the first 5 minutes is in a range between 6 and 14%, increasing gradually until 90 minutes and then it stabilizes.
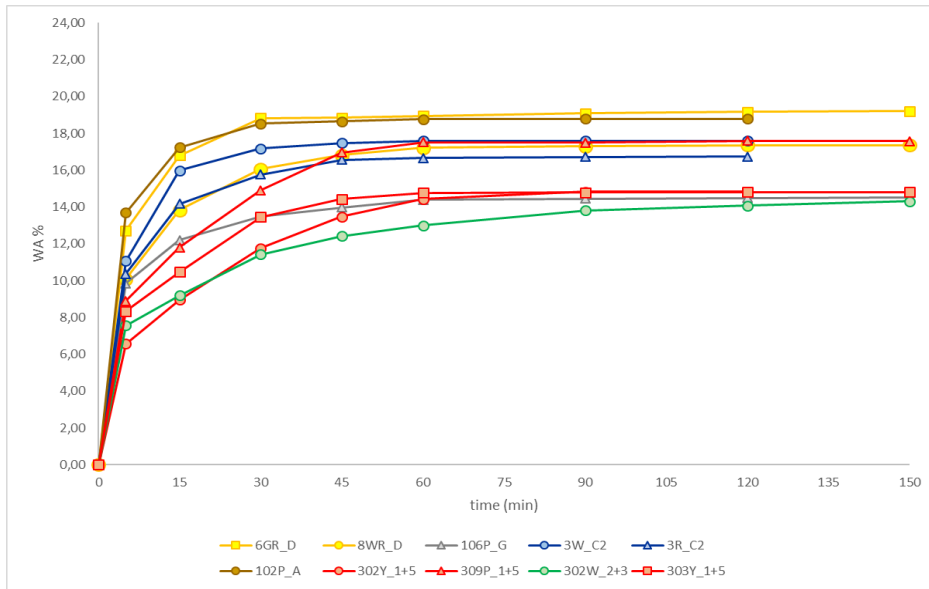
Figure 25. Absorption curves, Trend 1

Trend 2 shows a different pattern: the major absorption occurs within 5 minutes with a value around 19% for the *concotto* samples and 31% for the *incannucciato,* then increases slowly by ~0.4% until saturation, suggesting a similar porosity between samples 307P_2, 328W_4, 309BL_4 and 26OR_F.
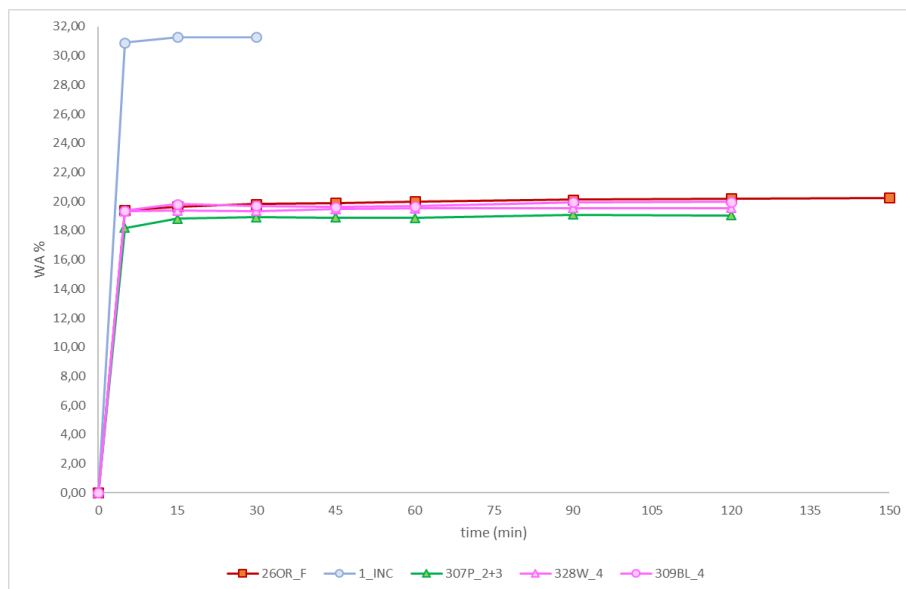
Figure 26. Absorption curves, Trend 2

Trend 3 shows an absorption value between 14 and 19% in the first 5 minutes, increasing by ~3% after 10 minutes and stabilizing until saturation.
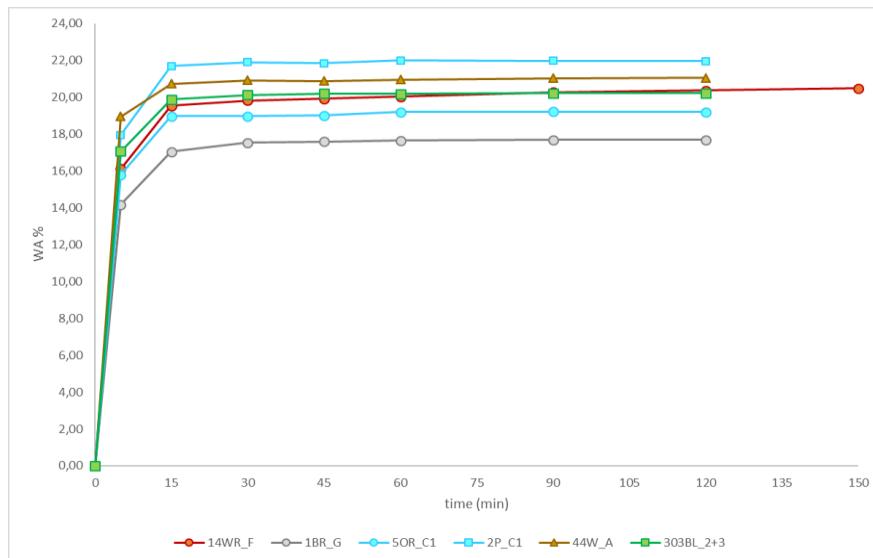
Figure 27. Absorption curves, Trend 3

Considering the curves, groups C2, 1+5 and D revealed the same trend (1), group 4 fitted Trend 2 and group C1 Trend 3. Samples from groups 2+3, F and G do not have a common pattern.

Depending on the absorption rate the dimension of pores can be supposed (Gane, et al., 2004). Since Trend 2 is characterized by a high absorption rate, samples following this trend are supposed to have small pores. On the other hand, samples following Trend 1 should have bigger pores.

In addition, draying values were also considered. After reaching water saturation, samples have been left to dry at room temperature, recording the weight after 3-5, 24 and 48 hours. Two representative samples are shown in Figure 28 ,while 1_INC reveals a different trend displaying a more rapid drying rate (Figure 29) confirming the high porosity suggested above. Furthermore, sample 14W and 6GR present a slower desorption rate (Figure 30), implying a lower porosity strengthened by the fact that these two fragments needed 7 hours to reach saturation. This feature could be a consequence of several factors, such as a different composition and/or a dissimilar production technique, as well as a different firing temperature compared to *concotto* samples.
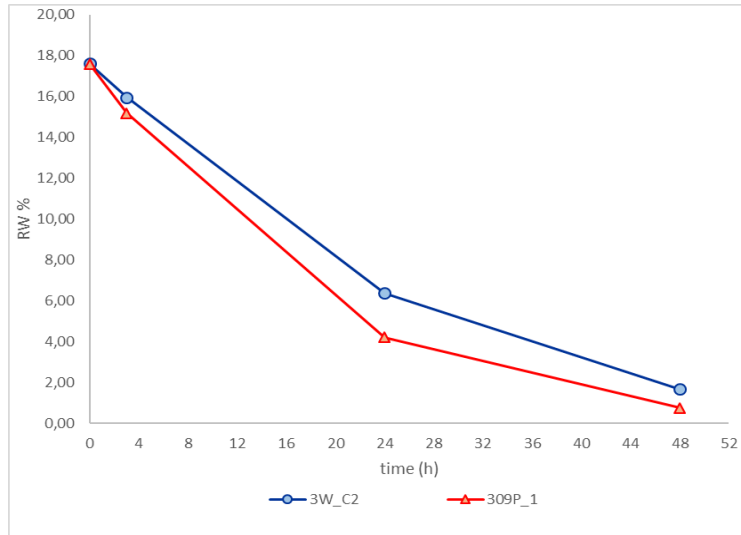
Figure 28. Representative drying curves
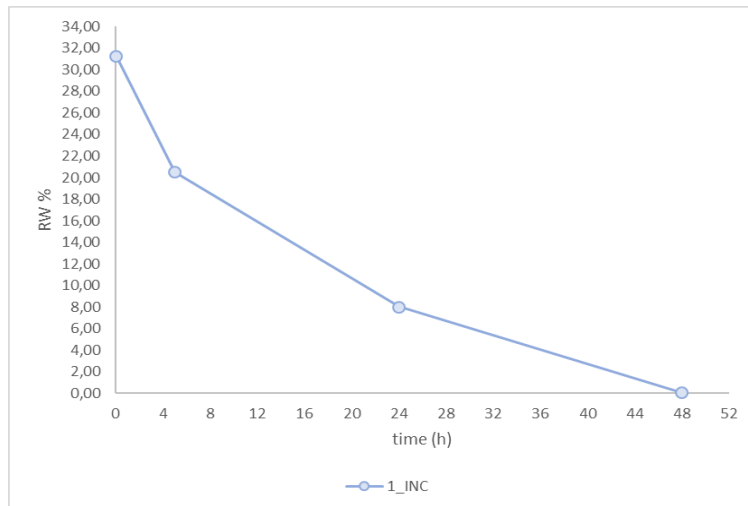
Figure 29. 1_INC drying curve
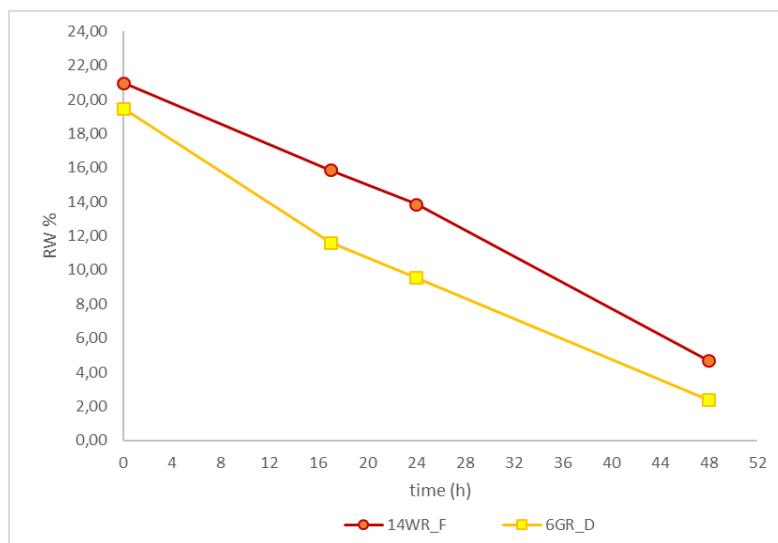
Figure 30. 14W and 6GR drying curves

3.3 FTIR and ATR spectroscopy results

FTIR spectroscopy allowed the identification of the chemical composition of the samples and the most representative spectra are showed in Figures 31-41.

Both sides of samples were analysed, as well as areas that differ in colour on the same surface, in order to recognise some similarities or discrepancies. The assignment was made by comparing the observed absorption frequencies with data available in literature, noting that ceramic samples were mainly composed of quartz, feldspars (orthoclase, albite), iron oxides (hematite and magnetite) and clay minerals (kaolinite and montmorillonite).

Similarities were detected in almost all spectra related to samples from groups C1, C2, 1, 2, 3 and 5, with the only distinction regarding the presence of hematite and magnetite. This consideration was confirmed by the surface colour, reddish or dark, respectively.

Figure 31 displays the FTIR spectrum of sample 303Y (side A, group 5), chosen as the representative for most of the ceramic artefacts analysed.

Quartz can be identified by the shoulder at 1164 cm^{-1} and the maximum peak at 986 cm^{-1} both related to the asymmetric stretching mode of Si-O groups, the characteristic doublet assigned to the symmetric stretch of Si-O at 796 and 778 cm^{-1}, the peak at 698 cm^{-1} due to the symmetric Si-O bending vibration and the peak at 448 cm^{-1} that refers to Si-O deformation (Müller, et al., 2014; Ravisankar, et al., 2010).

From the feldspar group, orthoclase can be detected by the peak at 643 cm^{-1} assigned to the Al-O coordination vibration (Ramasamy & Suresh, 2009), and albite from the peak at 721 cm^{-1} related to the Al-O-Si bending (Annamalai, et al., 2014).

Iron oxides have been also recognised providing some hints about firing conditions of the production of the *concotto* samples. The peak at 672 cm^{-1} in Figure 32 and the shoulder at 556 cm^{-1} in Figure 31 are ascribed to magnetite and hematite, respectively. Hematite peak is representative for pinkish and reddish surfaces, on the other hand magnetite was observed in some greyish spots. The presence of the former (hematite, Fe_2O_3) suggests an oxidizing atmosphere giving a red colouration to the material, whereas the latter (magnetite, Fe_3O_4) a reducing one producing a dark-grey colour (Ravisankar, et al., 2010; Velraj, et al., 2012).

Regarding clay minerals, a broad absorption band at 3500÷3000 cm^{-1}, centred around 3378 cm^{-1} for the sample 303Y, can be attributed to H-O-H stretching of water molecules in the interlayer of montmorillonite (Ravisankar, et al., 2010). Moreover, the peak at around 1636 cm^{-1} is related to the OH deformation of water (Müller, et al., 2014). In addition, in some spectra, as that in Figure 32, a peak at around 3624 cm^{-1} were detected suggesting the presence of kaolinite, referring to the vibrations of inner hydroxyl groups, lying between the tetrahedral and octahedral sheets, even if the

further three characteristic bands (3695, 3669, 3653 cm^{-1}) concerning the stretching vibrations of surface hydroxyl groups were not evident (Madejova, 2003; Djomgoue & Njopwouo, 2013).
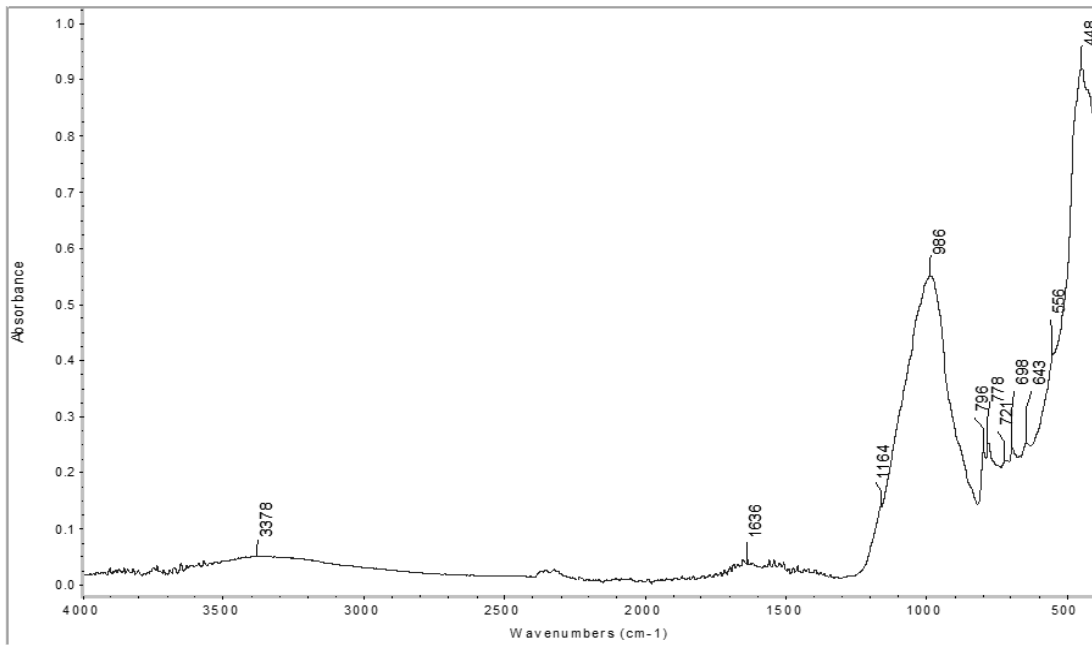
Figure 31. FTIR-ATR spectrum of 303Y_5 sample; side A, red.
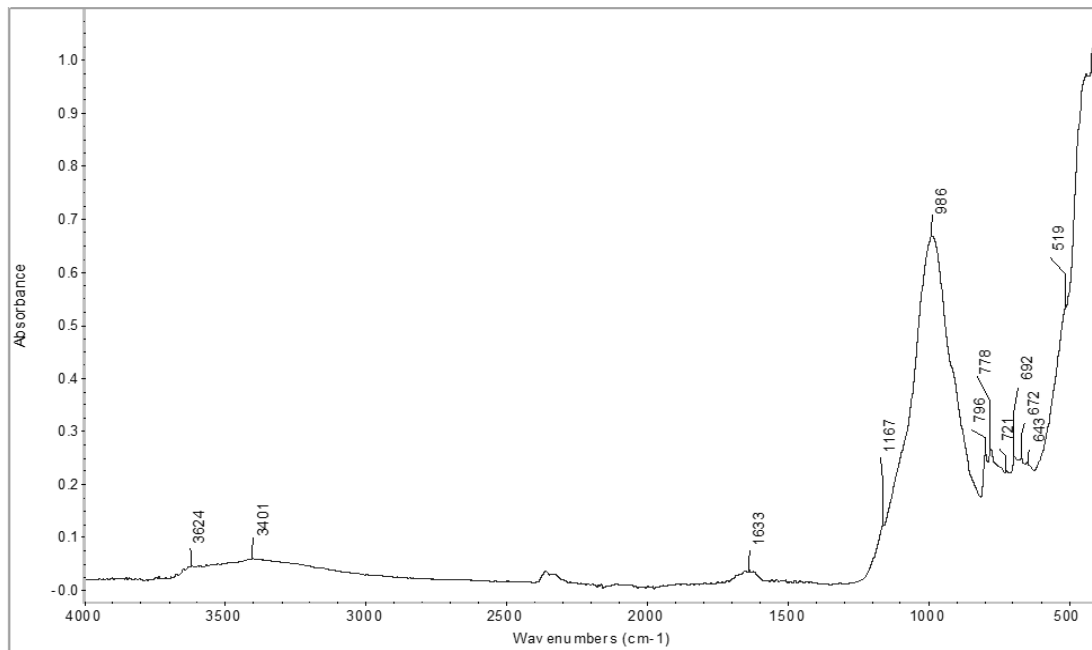
Figure 32. FTIR-ATR spectrum of 20Y_C2 sample; side B, dark spot.

Spectra from groups A and 4 presented different characteristic that could be related to different firing temperature.

Figure 33 represents the spectrum of sample 41W with no evidence of the 3500÷3000 cm^{-1} montmorillonite band, feature identified in all the samples from group A. Moreover, spectra from group A displayed a weak peak at around 872 cm^{-1} related to the Fe(AlOH) group in iron-rich clay minerals, and a weak shoulder at 918 cm^{-1} ascribable to Al-Al-OH bending vibration that could represent the presence of illite (Müller, et al., 2014; Alver, et al., 2016) but also kaolinite, since both are hydrated aluminum silicates (Djomgoue & Njopwouo, 2013). Characteristic of groups A is also the peak at 504 cm^{-1} related to diopside (De Benedetto, et al., 2002).
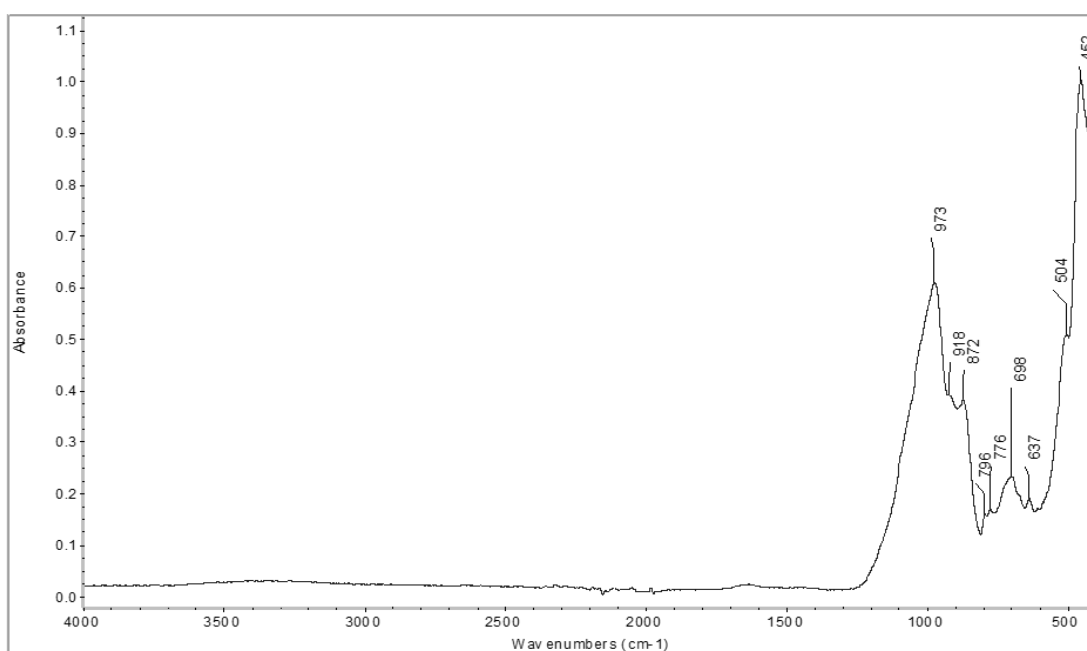
Figure 33. FTIR-ATR 41W_A sample; side A, black.

Concerning group 4, Figure 34 presents sample 304P spectrum, in which the Fe(AlOH) peak at 879 cm^{-1} is sharper compared to that of group A. The peak at 608 cm^{-1} can be attributed to the Mg$_3$OH bending of chrysotile (Mg$_3$(Si$_2$O$_5$)(OH)$_4$), a silicate mineral belonging to the subgroup of phyllosilicates (Madejova, 2003). In addition, quartz (985, 796 and 776 cm^{-1}) montmorillonite (3369 and 1636 cm^{-1}), feldspar (718 cm^{-1}), magnetite (675 cm^{-1}) and diopside (504 cm^{-1}) were identified.
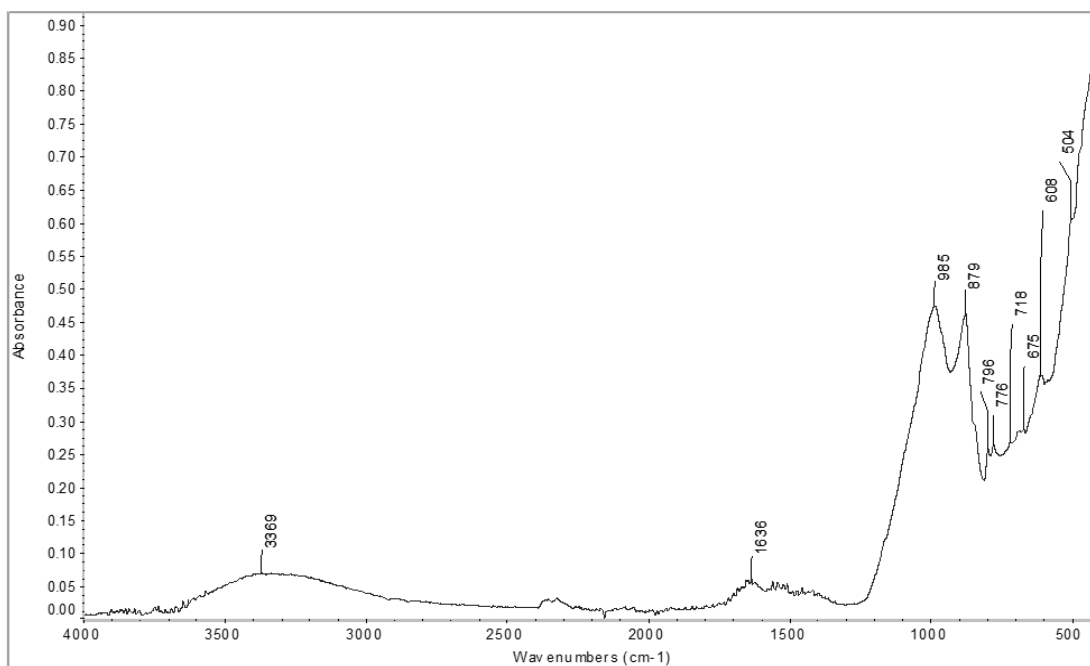
Figure 34. FT IR-ATR spectrum of 304P_4 sample; side B, light brown

Few spectra (group 6) display distinctive peak of gypsum. Figure 35 shows sample 323W spectrum, in which almost all the vibration signals identify the presence of gypsum: bands at 3524, 3400 and 3236 cm^{-1} refer to the O-H stretching vibration, the O-H-O bending well defined peaks at 1683 and 1620 cm^{-1}, the S-O stretching of sulphates at 1108 and 1005 cm^{-1}, and the S-O bending of sulphates at 669, 598, 441 and 419 cm^{-1} (lisa.chem.ut.ee, s.d.). The presence of quartz is also confirmed by the doublet at 796 and 776 cm^{-1}.
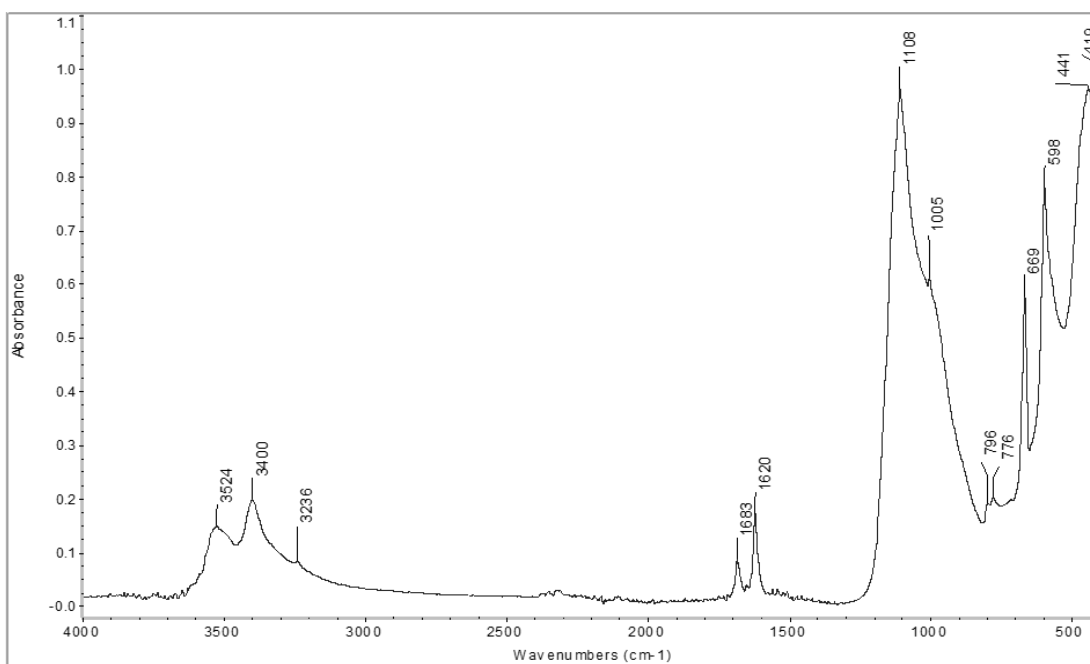
Figure 35. FT IR-ATR spectrum of 323W_5 sample; side A, rusty red

Moreover, additional FTIR analysis were performed in transmittance mode, supporting few micrograms of sample in a KBr pellet.

Superficial and bulk composition of sample 367BL_6 was examined in order to understand the nature and the distribution of the efflorescence noticed by naked eye. Side A spectrum revealed vibration signals characteristic of gypsum, as for sample 323W_5. Meanwhile, Figure 36 shows the transmittance bulk spectrum in which quartz (1167, 1036, 797, 779, 694 cm^{-1}) and feldspar (724, 646 cm^{-1}) are recognised. The peak at 3409 cm^{-1} and the shoulders at 3546 cm^{-1} and 3242 cm^{-1} are related to H-O-H stretching of water molecules which could derive from both montmorillonite and gypsum, as for the O-H-O bending at 1623 cm^{-1} , even if no other vibrational signs of gypsum have been detected. The peak at 475 cm^{-1} can be ascribed to hematite (Ravisankar, et al., 2010; Barone, et al., 2011), however it could also be related to kaolinite, as for the shoulder at 3630 cm^{-1} and the absorption band at 1036 cm^{-1} overlapped with silicates band (Ravisankar, et al., 2010). Furthermore, the two weak bands observed at 2921 cm^{-1} and 2848 cm^{-1} can be attributed to C-H vibration, probably originated from organic matter (Müller, et al., 2014; Singh & Sharma, 2016).
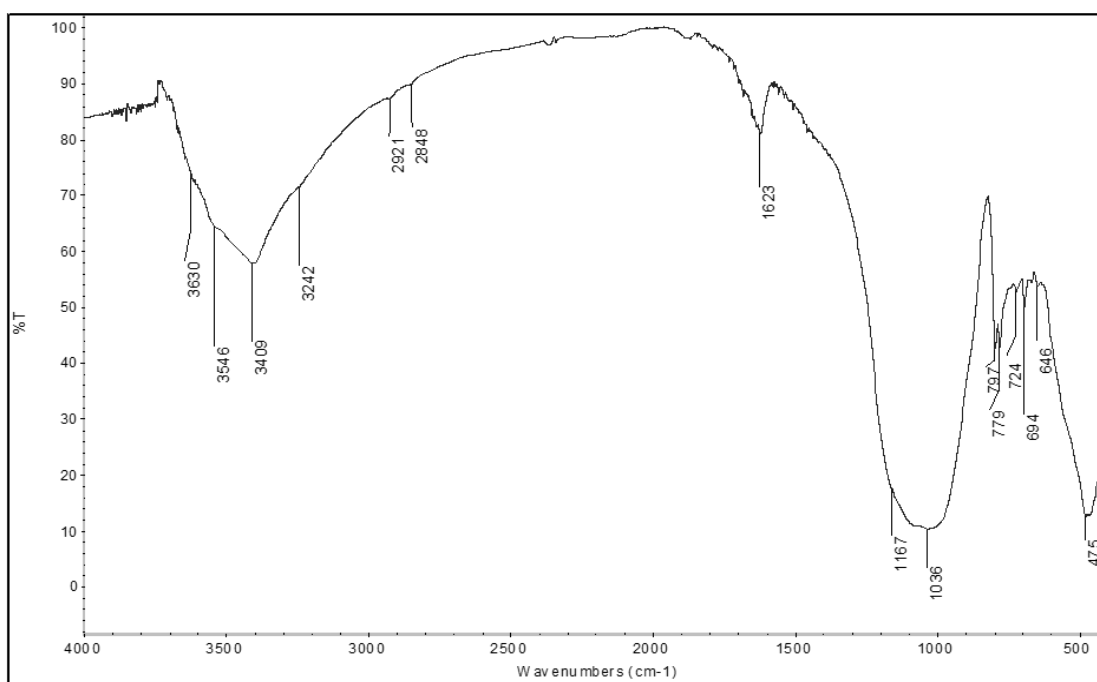
Figure 36. FT IR spectrum of 367BL_6 sample; bulk

As previously observed through OM analysis, sample 41W presented different layers, which may be due to various firing temperature. For this reason, the bulk of sample 41W_A was analysed in order to determine similarities with FTIR-ATR spectrum in Figure 33, especially to evaluate the presence of diopside. Figure 37 does not display the characteristic peak at ~504 cm^{-1} related to diopside. Moreover, it shows peak of montmorillonite (3424 and 1618 cm^{-1}), as well as quartz (1162, 1027,

777 and 698 cm^{-1}), hematite (538 and 462 cm^{-1}) and feldspar, such as albite (728 and 741 cm^{-1}) and K-feldspar such as orthoclase (629 cm^{-1}), and microcline at 581 cm^{-1} corresponding to the O-Si-(Al)-O bending vibration (Ramasamy & Suresh, 2009).
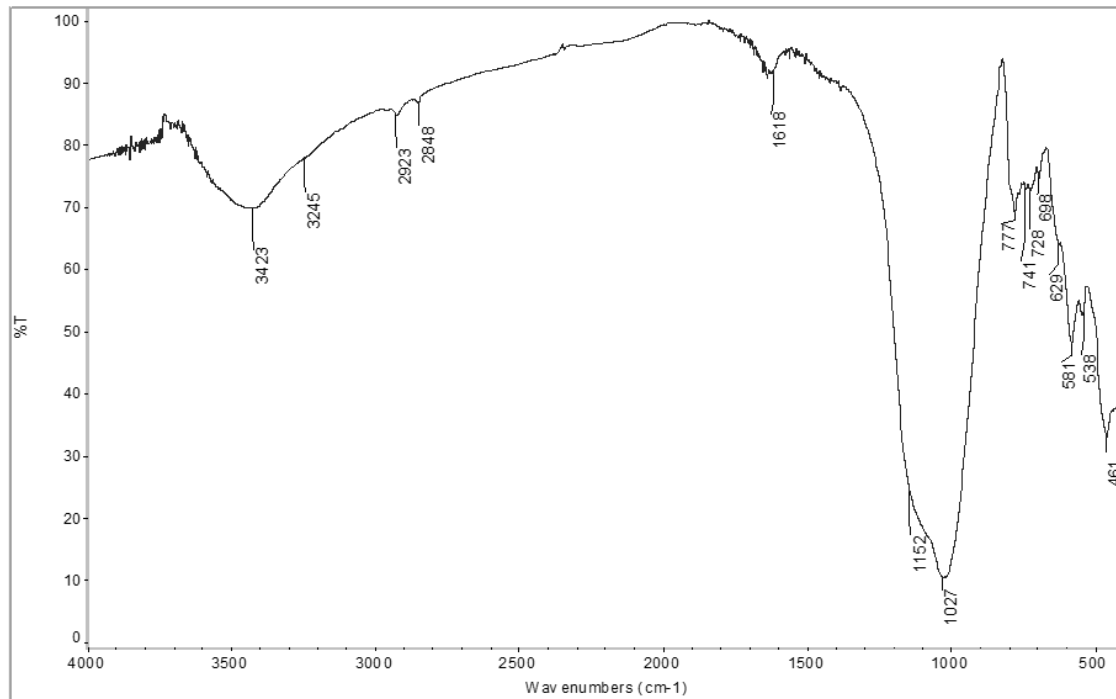
Figure 37. FT-IR spectrum of 41W_A sample; bulk

Samples form group D, F and G, that show a particular morphology, were also analysed in order to determine similarities or discrepancies compared to *concotto* samples.

Figure 38 displays the spectrum of sample 106P_G, in which quartz (1167, 1028, 798, 779 and 694 cm^{-1}), feldspar (724, 715, 646 cm^{-1}), montmorillonite (3424, 3223, 1636 and 527 cm^{-1}) have been identified, as well as the weak shoulders at 872 cm^{-1} ascribable to the Fe(AlOH) group and at 906 cm^{-1} related to Al-Al-OH bending vibration. As for 367BL_6 spectrum, the peak at 473 cm^{-1} can be ascribed to hematite or kaolinite, given the presence of 1028 and 3621 cm^{-1} peaks. The main feature that characterised this spectrum, which is representative also for samples 1BR_G, 6GR_D and 14WR_F, is the presence of 1421 and 1795 cm^{-1} vibrations concerning -CO_3 stretching mode and carbonyl group (C=O) respectively, ascribable to calcite (Ravisankar, et al., 2010; lisa.chem.ut.ee, s.d.). Moreover, the peak at 2921 and 2848 cm^{-1} can be attributed to asymmetrical and symmetrical CH_2 stretching of carbonates, respectively (Bruckman & Wriessnig, 2013).
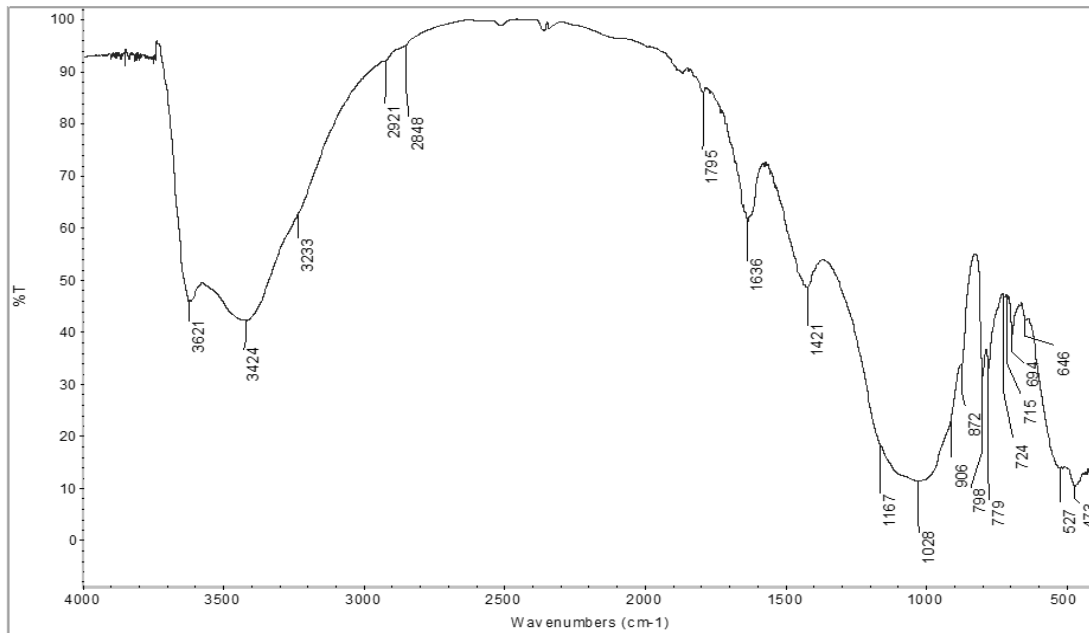
Figure 38. FT IR spectrum of 106P_G sample; bulk

Spectrum concerning the external whiteish side of sample 14WR_F is shown in Figure 39, reporting quartz (1077, 1031, 770 and 697 cm⁻¹), calcite (2921, 2845 and 1437 cm⁻¹) and feldspar (715 and 636 cm⁻¹). As previously explained for sample 367BL_6, peaks at 3551, 3482, 3416 cm⁻¹ and the shoulder at 3230 cm⁻¹ are related to H-O-H stretching of water molecules ascribable to both montmorillonite and gypsum, as for the O-H-O bending at 1637 cm⁻¹. Moreover, the weak peak at 669 cm⁻¹ are related to gypsum. Even in this case the peak at 472 cm⁻¹ can refer to hematite or kaolinite. Furthermore, 918 and 872 cm⁻¹ vibration peaks are more define as for sample 41W_A. An additional similarity to sample 41W_A is the presence of the diopside peak at 510 cm⁻¹.
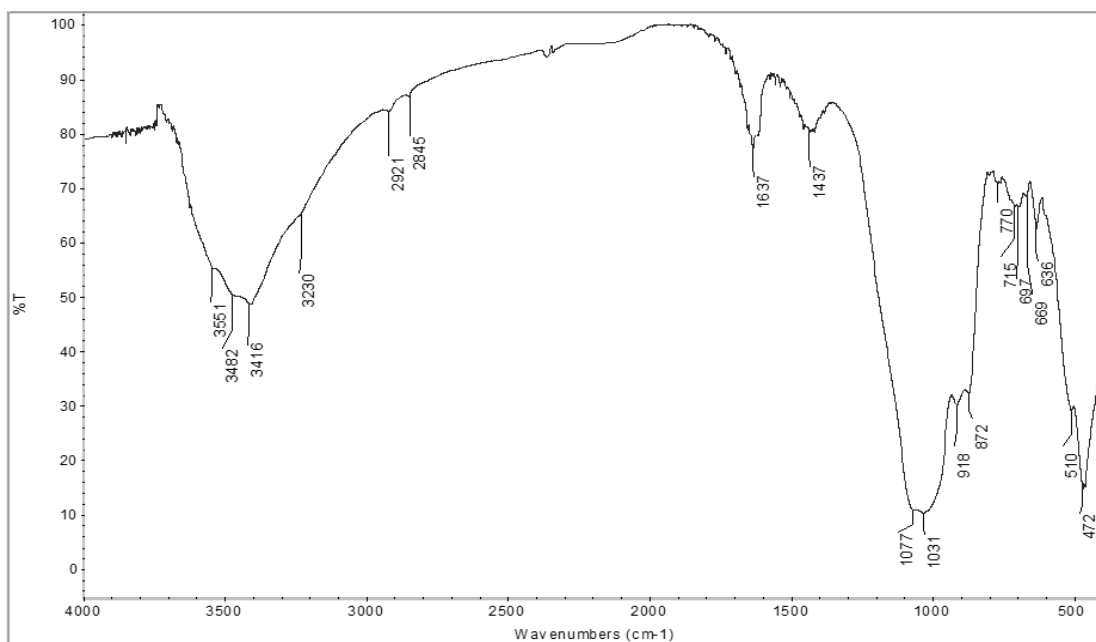
Figure 39. FT IR spectrum of 14WR_F sample; ext whiteish

Figure 40 represents the spectrum of *incannucciato* sample (1_INC), reporting quartz (1048, 796, 776 and 689 cm^{-1}), feldspar (713, 649 and 467 cm^{-1}), calcite (2918, 2851, 1789 and 1453 cm^{-1}), montmorillonite (3424, 3236 and 1636 cm^{-1}), hematite (556 cm^{-1}) and the Fe(AlOH) vibration at 875 cm^{-1}.
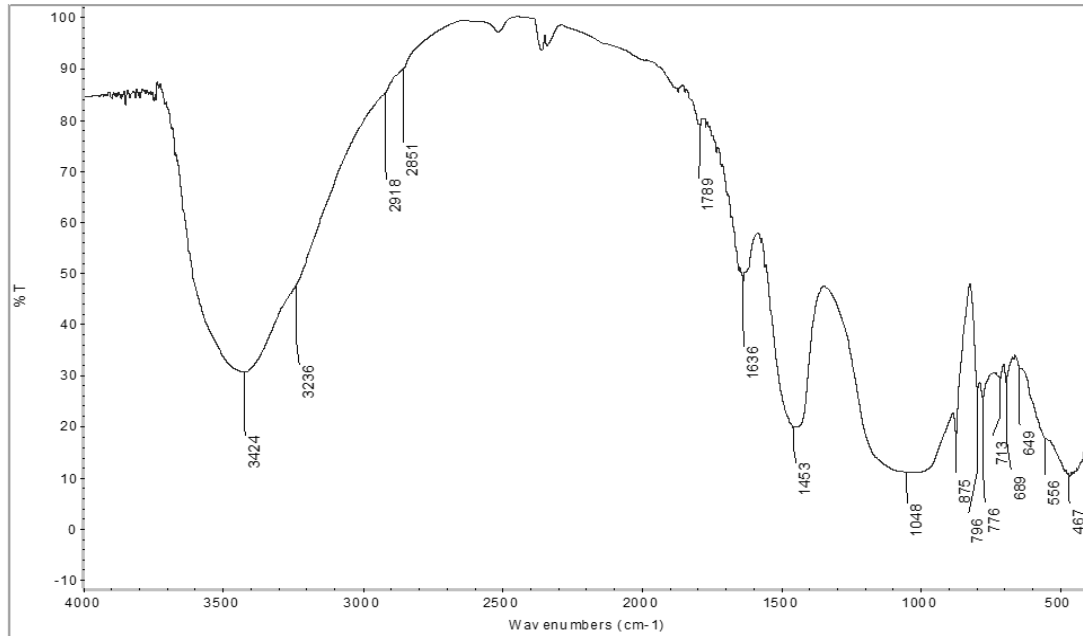
Figure 40. FT-IR spectrum of 1_INC sample

In order to unsure the presence of calcite, an additional analysis was performed. The sample was treated with hydrochloric acid (HCl) to induce the release of CO_2, and after several water rinses and a drying period, it was examined by FT-IR spectroscopy. The spectrum in Figure 41 shows a less pronounced peak of calcite at 1424 cm^{-1}.
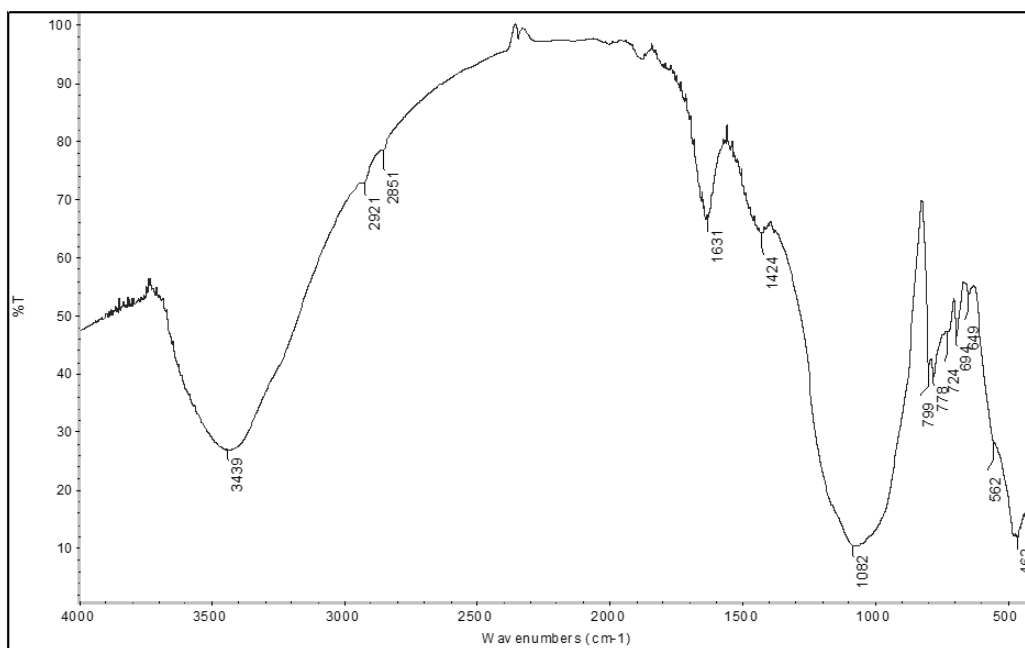
Figure 41. FT-IR spectrum of 1_INC after HCl treatment

Based on the IR spectroscopic results, some general considerations about the chemical composition of ceramics can be defined:

- almost all the samples appear to be composed of silicates as quartz and feldspars (orthoclase, albite), iron oxides (hematite and magnetite) and clay minerals (kaolinite and montmorillonite);

- in addition, samples from group 4 and A present iron-rich clay minerals signals and diopside vibration in the surface, but not in the bulk;

- illite is found only in group A, as well as chrysotile is present only in group 4;

- samples from group 6 display an evident presence of gypsum on the surface and a more heterogeneous composition of the bulk;

- calcite appears in samples from group G, D and F;

Concerning the *incannucciato* sample, the chemical composition is characterized by silicates, clay minerals, iron oxides and calcite.

The presence of hematite asserts a prevalent oxidizing atmosphere at the time of manufacture process. Furthermore, the presence or absence of some vibrational bands in the IR spectra allows to draw some conclusion on the firing temperature:

- the presence of kaolinite signals submits a low process temperature, since it turns to metakaolinite through a dehydroxylation process between 450 and 650°C (Kurap, et al., 2010);

- the presence of Al-Al(OH) vibration bands at 915 cm^{-1} suggests that samples have been fired below 500°C at the time of manufacture, since the octahedral sheet structure collapses completely near 500°C (Singh & Sharma, 2016; Velraj, et al., 2012);

- illite vibrational bands suggests a temperature below 700°C, since its structure begins to break down between 700 and 850°C (Stevenson & Gurnick, 2016);

- the presence of the montmorillonite band at around 3400 cm^{-1} suggests that the ceramic fragments were produced at a temperature below than 800°C, which is the limit temperature at which the mineral undergoes dehydroxylation (Ravisankar, et al., 2010);

- the presence of calcite indicates a firing temperature below its decomposition temperature of 720÷900°C (Akyuz, et al., 2008);

- above 800°C high-temperature crystalline phase formation is promoted and the presence of diopside suggests a high process temperature (Ravisankar, et al., 2010).

3.4 TGA-DSC results

TGA analysis is very important for the determination of firing temperature of archaeological ceramics. TGA–DSC curves were examined considering both the heat flow of samples and the mass loss expressed as percentage, both as function of temperature.

In the following thermograms exothermic peaks are directed downwards.

The presence of an endothermic peak for a known mineral suggests that the ceramic has never been fired to that temperature before; on the contrary, its absence indicates that sample has been fired to at least that temperature (Leach, et al., 2008).

The TGA results expressed as percentage of mass loss are shown in Table 19 considering different temperature ranges. Each range can be correlated to specific chemical reactions as follows (Cuomo di Caprio, 2007; Leach, et al., 2008), corresponding to a weight loss:

- <100°C: an endothermic peak in this range indicates the loss of moisture water;

- 100-200°C: an endothermic peak is due to the loss of absorbed water;

- 200-400°C: an exothermic peak in this range is related to the combustion of organic material;

- 400-600°C: an endothermic peak in this range indicates the loss of chemically combined hydroxyl water by clay minerals;

- >600°C: an endothermic peak is due to the decomposition of calcite, and an exothermic peak at about 900°C is related to the formation of high temperature phases form clay minerals.

Moreover, Table 20 evidences the total weight loss for each sample.

Based on the previous results, few selected samples were chosen in the interest of correlating the firing temperatures with specific groups. Samples considered were: 367BL_6 (bulk), 328BL_6 (side A), 2P_C1 (side A), 309P_1 (bulk), 41W_A (bulk), 106P_G (bulk) and 1_INC (bulk).

In order to better understand the presence of gypsum in samples from group 6, TGA-DSC analyses were performed on few mg of powder from side A of sample 367BL and from the bulk of sample 328BL. Figure 42 shows a sharp endothermic DSC peak at 140.3°C referring to the loss of water, followed by a weight loss of 12.59%, that can be ascribed to gypsum (Moropoulou, et al., 1995). Moreover, the weak shoulder at 341.8°C referred to water loss in iron hydroxides (Moropoulou, et al., 1995).
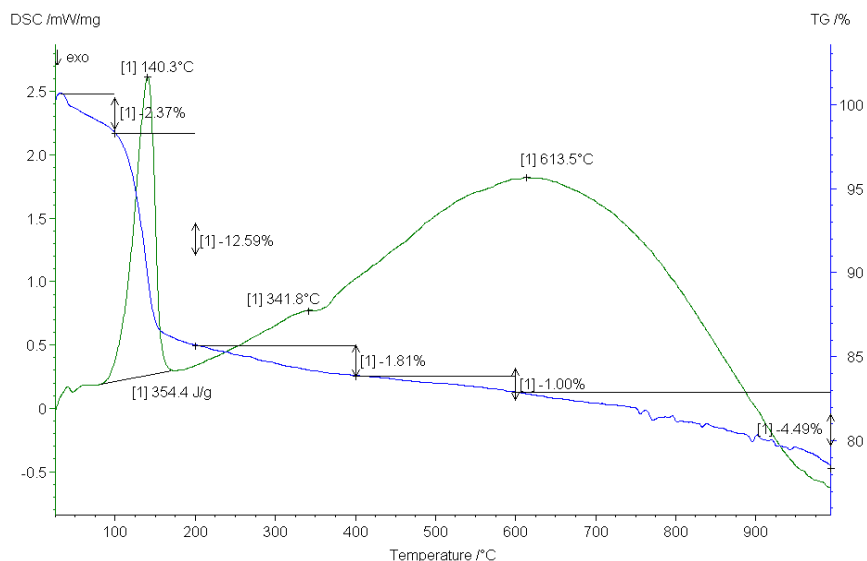
Figure 42. TG-DSC thermogram of sample 367BL_6_side A

Furthermore, no other thermograms display the same feature, not even the 328BL bulk analysis (Figure 43), suggesting that the presence of this mineral is a superficial characteristic of samples from group 6. Meanwhile, the weak peak at 117.1°C in Figure 43 is related to the dehydroxylation of physically absorbed water and the interstitial water (Alver, et al., 2016).

An endothermic peak around 550÷650°C indicates the loss of hydroxyl water by clay minerals (Leach, et al., 2008; Moropoulou, et al., 1995). Since a broad peak in this region is present in all the thermograms, except for 1_INC, it is difficult to attribute the dehydroxylation phase to one precise clay mineral. Kaolinite is characterised by two major endothermic peaks relates to dehydroxylation between 500°C and 600°C and one exothermic peak at 950°C referring to the complete conversion to metakaolinite (Diko, et al., 2016; Stevenson & Gurnick, 2016), but this latter is absent in all the samples. Montmorillonite dehydroxylates around 500-550°C and crystalline structure of illite starts to break down at 700°C (Stevenson & Gurnick, 2016).
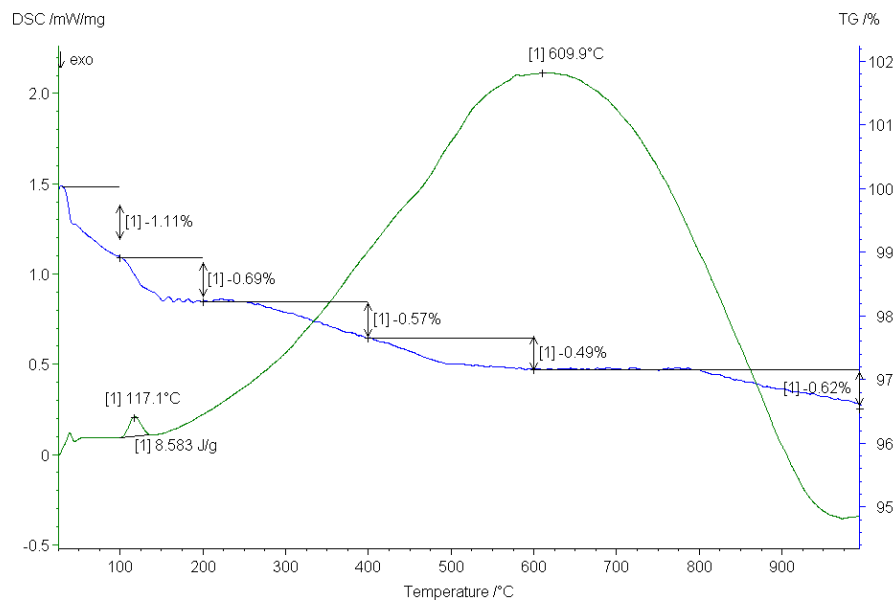
Figure 43. TG-DSC thermogram of sample 328BL_6_bulk

Figure 44 reports the TGA-DSC curves concerning sample 1_INC, which seems to show differences from the others. The DSC peak at 576.9°C refers to the polymorph transformation of α- to β-quartz (Mothé & Ambrosio, 2007), while the peak at 684.3°C could be ascribable to the decomposition of calcite, accompanied by a weight loss of 4.25 % (Table 19).Generally, peak temperature for $CaCO_3$ vary from 860 to 1010°C (Mackenzie, 1970), however in some cases decomposition occurred at lower temperature (Bakolas, et al., 1995; Fabbri & Fiori, 1987).
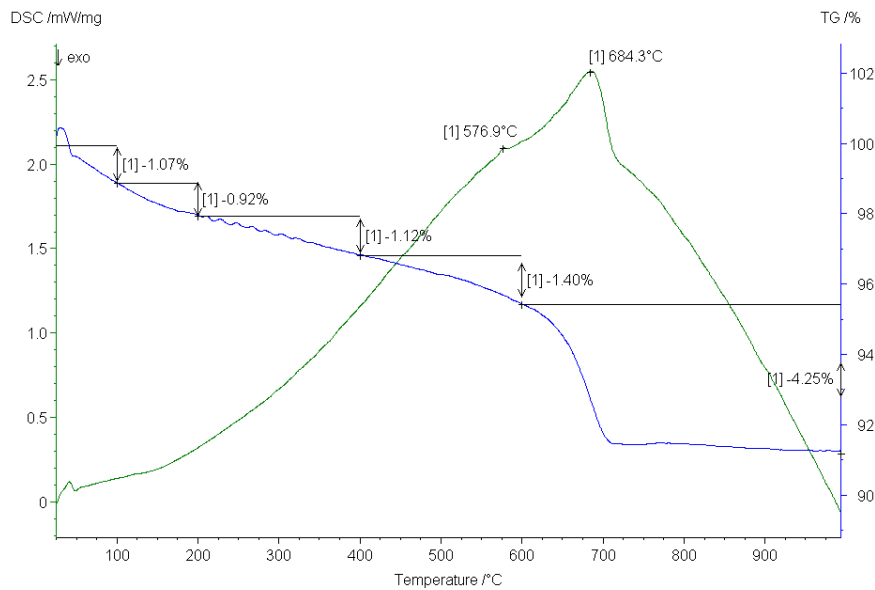
Figure 44. TG-DSC thermogram of sample 1_INC_bulk

To confirm this result sample 1_INC after HCl treatment was analysed. The thermogram in Figure 45 does not display the same peak and mass loss after 600°C as Figure 44, confirming on this latter the presence of calcite.
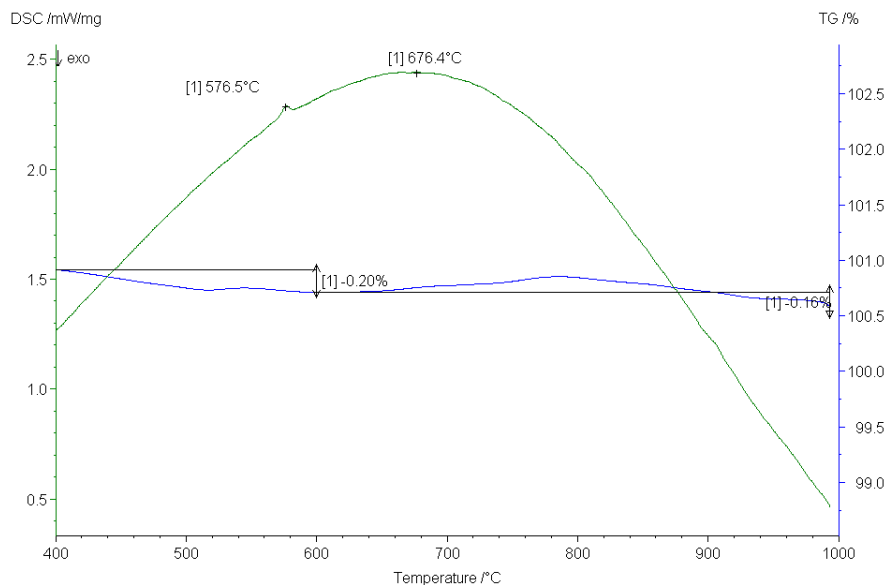
Figure 45. TGA-DSC curves of sample 1_INC bulk after HCl treatment. Temperature range between 400 and 1000°C.

In addition, Table 19 shows the percentage of weight loss per temperature range and Table 20 displays the total weight loss (%) in order to compare these values between all samples analysed. A significant characteristic has been detected in Sample 367BL_6, which presented the highest values suggesting a clear difference in composition attributable to the presence of gypsum.

Table 19. Percentage of mass losses per temperature range.

Sample	<100°C	100-200°C	200-400°c	400-600°C	>600°C
367BL_6	-2.37%	-12.59%	-1.81%	-1.00%	-4.49%
328BL_6	-1.11%	-0.69%	-0.57%	-0.49%	-0.62%
2P_C1	-1.14%	-1.74%	-1.70%	-0.68%	-1.55%
309P_1	-1.09%	-0.07%	-0.47%	-0.67%	-0.42%
41W_A	-0.17%	-0.62%	-0.69%	-0.35%	-0.78%
106P_G	-1.02%	-0.21%	-0.76%	-1.92%	-1.79%
1_INC	-1.07%	-0.92%	-1.12%	-1.40%	-4.25%

Table 20. Total weight loss results

Sample	367BL_6	328BL_6	2P_C1	309P_1	41W_A	106P_G	1_INC
Total weight loss	22.26 %	3.48 %	6.81 %	2.72 %	2.61 %	5.70 %	8.74 %

According to these results, the firing temperature of all the ceramic fragments and of *incannucciato* sample should have been lower than 500°C, despite the preliminarily subdivision in groups.

4 CONCLUSIONS

Aim of the study was the characterisation of non-vascular ceramic materials found in two distinct Etruscan settlements: San Basilio and Adria, both situated in the Po Delta region (north Italy).

A multi-analytical approach was carried out using specific investigation methods such as Fourier-transform infrared (FTIR) and ATR mode spectroscopies, thermogravimetry coupled with differential scanning calorimetry (TGA-DSC), stereo-microscopic observations of cross sections and evaluation of the open porosity. This approach allowed to collect useful results about the composition of ceramic mixtures, as well as the methodology of firing, suggesting interesting hypothesis about the role of these materials within the construction process.

Preliminary observations by naked eye and by digital microscope allowed to subdivide all fragments in several groups basing on morphological features and colours. The subsequent aim was to understand if there were some compositional differences between groups and sites; *in-situ* FTIR-ATR spectroscopy allowed the analysis of a great part of the ceramic pieces in order to identify the most characteristic samples. These latter were then subjected to additional investigation in order to obtain information about the firing process techniques.

The obtained results gave information about the chemical composition, showing that the main components of *concotto* fragments were silicates (quartz and feldspar), clay minerals (kaolinite and montmorillonite) and iron oxides (hematite and magnetite). A particular feature concerned samples from groups 4 and A, which displayed the superficial presence of diopside, a mineral that can be naturally present in the ceramic body, but whose formation is generally promoted at high temperature (>800°C). In addition, stereomicroscopic observations manifested the evidence of a layered bulk, suggesting that only the superficial part of that samples underwent to high temperatures. This was confirmed also by TGA-DSC results, indicating a firing temperature of the bulk below 500°C. It can be deduced that, unlike the others, these fragments underwent to a superficial high-temperature fire phenomenon.

Optical observations and FTIR spectroscopic analyses demonstrated the presence of gypsum predominantly on the surface of samples from group 6, implying a depositional formation of the efflorescence due to environmental conditions more than to compositional features.

Moreover, samples from group F seemed to be part of silos and presented a greyish cover layer that could be intentionally applied as coating by the producer. Slow absorption and desorption rates suggested a low porosity of the material.

In addition to the ceramic fragments, several portions of daub were found in San Basilio site, being characterized by reeds and branches impressions, suggesting the wattle and daub construction technology for the realization of the domestic walls. These *incannucciato* samples presented a

chemical composition rich in silicates, clay minerals, iron oxides and calcite. The presence of this latter was observed in the TGA-DSC curve as well, while the transformation of α- to β-quartz suggested also in this case a production temperature below 500°C. *Incannucciato* fragments showed the highest values of water absorption, revealing a high open porosity and the presence of small pores compared to *concotto* samples.

All of these archaeological findings are supposed to be building materials used for covering house walls, as external or internal plasters. Similar materials were found also in Spina settlement, explaining the role of *concotto* as plasters used in the bottom part of the wall being more water-resistant, and the use of *incannucciato* daub fragments to cover the upper part of the wattle structure (Zamboni, 2016). Since low water absorption values imply good resistance to the natural environment and a good permeability (Aouba, et al., 2016), this study can confirm the interpretation of Zamboni (2016).

Further research might be done on vascular ceramic findings coming from the same archaeological sites, comparing chemical compositions and firing temperatures in order to detect similarities or differences in the production process of both vascular and non-vascular potteries. In addition, a project of experimental archaeology could be developed to test the abovementioned archaeological hypotheses investigating the feasibility of ancient construction methods. These approaches would lead to clarify the ancient production processes of domestic construction materials in the Delta Po area during the 6th and 5th century BC.

Bibliography

Akyuz, S. et al., 2008. Analysis of ancient potteries using FT-IR, micro-Raman and EDXRF spectrometry. *Vibrational Spectroscopy,* Volume 48, pp. 276-280.

Alver, B. E., Dikmen, G. & Alver, O., 2016. Investigation of the influence of heat treatment on the structural properties of illite-rich còay mineral using FT-IR, 29Si MAS NMR, TG and DTA methods. *Anadolu University Journal of Science and Technology,* Volume 17, pp. 823-829.

Ammermann, A. J., Shaffer, G. D. & Nicholas, H., 1988. A Neolithic Household at Piana di Curinga, Italy. *Journal of Field Archaeology,* 15(2), pp. 121-140.

Annamalai, R. G. et al., 2014. Application of various spectroscopic techniques to characterize thearchaeological pottery excavated from Manaveli, Puducherry, India.. *Optik,* Issue 125, pp. 6375-6378.

Aouba, L. et al., 2016. Properties of fired clay bricks with incorporated biomasses: Cases of Olive Stone Flour and Wheat Straw residues. *Construction and Building Materials,* Volume 102, pp. 7-13.

Bakolas, A., Biscontin, G., Moropoulou, A. & Zendri, E., 1995. Physico-chemical characteristics of traditional mortars in Venice. In: *Proceedings Structural studies of historical buildings IV.* Southampton: Computational Mechanics Pubblications, pp. 187-194.

Barone, G. et al., 2011. FT-IR spectroscopic analysis to study the firing process fo prehistoric ceramics. *Journal of Molecular Structure,* Volume 993, pp. 147-150.

Battaglia, D. M., 2014. *Caratterizzazione e conservazione di reperti ceramici archeologici,* Master's degree thesis in Scienze Chimiche per la Conservazione e il Restauro: Ca' Foscari University of Venice.

Bayazit, M. et al., 2013. FT-IR spectroscopic analysis of potshreds excavated from the first settlement layer of Kuriki Mound, Turkey. *International Journal of Modern Physics,* Volume 22, pp. 130-111.

Bonomi, S., Callegher, B., Perini, L. & Ruzza, R., 2000. *Il sito archeologico di San Basilio: una storia ancora da scrivere.* Taglio di Po: Arti Grafiche Diemme.

Bruckman, V. J. & Wriessnig, K., 2013. Improved soil carbonate determination by FT-IR and X-ray analysis. *Environmental Chemistry Letters,* Volume 11, pp. 65-70.

Campanella, L. et al., 2007. *Chimica per l'arte.* Bologna: Zanichelli.

Camporeale, G., 1997. On Etruscan Origins, Again. *Etruscan and Italic Studies, Journal of the Etruscan Foundation,* Volume 4, pp. 45-51.

Cantisani, E. et al., 2012. Ceramic findings from the archaeological site at Aiano-Torraccia di Chiusi (Siena, Italy): a multi-analytical approach. *Archaeological and Anthropological Sciences,* Volume 4, pp. 29-46.

Croce, E., Amicone, S., Castellano, L. & Vezzoli, G., 2014. Analisi di una tecnica edilizia in terra cruda nell'insediamento etrusco-padano del Forcello di Bagnolo San Vito (Mantova). *Notizie Archeologiche Bergomensi,* Issue 22, pp. 137-160.

Cuomo di Caprio, N., 2007. *Ceramica in Archeologia 2: antiche tecniche di lavorazione e moderni metodi di indagine.* Roma: "L'ERMA" di BRENTSCHNEIDER.

De Benedetto, G., Laviano, R., Sabbatini, L. & Zambonin, P., 2002. Infrared spectroscopy in the mineralogical characterization. *Journal of Cultural Heritage,* Volume 3, pp. 177-186.

De Min, M., 1984. Adria Antica. In: *Il Veneto nell'antichità. Preistoria e protostoria..* Verona: Banca Popolare di Verona, pp. 809-830.

De Min, M., 1986. L'abitato arcaico di S. Basilio di Ariano Polesine. In: *L' antico Polesine : testimonianze archeologiche e paleoambientali.* Padova: ., pp. 171-184.

De Min, M., 1986. L'abitato arcaico di S. Basilio di Ariano Polesine. In: *L' antico Polesine : testimonianze archeologiche e paleoambientali ; catalogo delle esposizioni di Adria e di Rovigo, febbraio - novembre 1986.* Adria: Museo Nazionale Archeologico di Adria, pp. 171-184.

De Min, M., 1988. Adria e il suo territorio in età preromana. In: *Gli Etruschi a nord del Po.* Regione Lombardia - Provincia e Comune di Mantova: Capannotto Editore.

De Min, M., 1988. L'abitato arcaico di S. Basilio. In: *Etruschi a nord del Po.* Regione Lombardia - Provincia e Comune di Mantova: Campanotto Editore, pp. 84-91.

Diko, M., Ekosse, G. & Ogola, J., 2016. Fourier Tensform Infrared Spectroscopy and Thermal Analyses fo Kaolinitic Clays from South Africa and Cameroon. *Acta Geodynamica Geomaterialia 13,* 2(182), pp. 149-158.

Djomgoue, P. & Njopwouo, D., 2013. FT-IR Spectroscopy Applied for Surface Clays Characterization. *Journal of Surface Engineered Materials and Advanced Technology,* Volume 3, pp. 275-282.

Drebushchak, V. A., Mylnikova, L. N., Drebushchak, T. N. & Boldyrev, V. V., 2005. The investigation of ancient pottery. Application of thermal analysis.. *Journal of Thermal Analysis and Calorimetry,* Volume 82, pp. 617-626.

Fabbri, B. & Fiori, C., 1987. Influence of sodium chloride on thermal reactions of heavy clays during firing. In: *Proceedings of the International Clay Conference, Denver, 1985.* Bloomington (Indiana): The Clay Minerals Society, pp. 319-395.

Fabbri, B., Gualtieri, S. & Shoval, S., 2014. The presence of calcite in archaeological ceramics. *Journal of the European Ceramic Society,* Volume 34, pp. 1899-1911.

Fogolari, G. & Scarfì, B. M., 1970. *Adria antica.* Venezia: Aflieri.

Gambacurta, G. & Zega, L., 2013. *Guide tematiche dei musei archeologiche del Veneto. Adria, Museo Archeologico Nazionale di Adria.* Venezia: Regione del Veneto.

Gane, P. A., Ridgway, C. J. & Schoelkopf, J., 2004. Absorption Rate and Volume Dependency on the Complexity of Porous Network Structures. *Transport in Porous Media,* Volume 54, pp. 79-106.

Genedy, M., Stormont, J., Matteo, E. & Taha, M. R., 2014. Examining Epoxy-based Nanocomposites in Wellbore Seal Repair for Effective CO2 Sequestration. *Energy Procedia,* Issue 63, pp. 5798-5807.

Grim, R. E. & Rowland, R. A., 1942. Differential thermal analyses of clay minerals and other hydrous materials. Part 1. *American Mineralogist,* 27(11), pp. 746-761.

Kato, T., Ohashi, K., Fuji, M. & Takahashi, M., 2008. Water absorption and retention of porous ceramics fabricated by waste resources. *Journal of the Ceramic Society of Japan,* 2(116), pp. 212-215.

Kiruba, S. & Ganesan, S., 2015. FT-IR and Micro-Raman spectroscopic studies of archaeological potteries recently excavated in Poompuhar, Tamilnadu, India. *Spectrochimica Acta Part A: Molecular and Biomolecural Spectroscopy,* Volume 145, pp. 594-597.

Klouzkova, A., Kohoutkova, M., Zemenova, P. & Mazac, Z., 2014. Characterisation of a prehistorical ceramic object. Moon-shaped idol, by means of thermal analysis. *Journal of Thermal Analysis and Calorimetry,* Volume 116, pp. 641-645.

Kurap, G. et al., 2010. FT-IR spectroscopic study of terra-cotta sarcophagi recently excavated in Ainos. *Journal of Molecular Structure,* Volume 976, pp. 161-167.

Leach, F. et al., 2008. The Physical and Mineralogical Characteristics of Pottery from Mochong, Rota, Mariana Islands. In: *Islands of Inquiry: Colonisation, seafaring and the archaeology of maritime landscapes.* Camberra: ANU Press, pp. 435-452.

lisa.chem.ut.ee, n.d. [Online]
Available at: http://lisa.chem.ut.ee/IR_spectra/paint/fillers/calcite
[Accessed 16 01 2020].

lisa.chem.ut.ee, n.d. [Online]
Available at: http://lisa.chem.ut.ee/IR_spectra/paint/fillers/gypsum/
[Accessed 16 01 2020].

Liu, H. et al., 2013. The difference of thermal stability between Fe-substituted palygorskite and Al-rich palygorskite. *Journal of Thermal Analysis and Calorimetry,* Issue 111, pp. 409-415.

Livingstone Smith, A., 2001. Bonfire II: The Return of Pottery Firing Temperatures. *Journal of Archaeological Science,* Volume 28, pp. 991-1003.

Mackenzie, R., 1970. *Differential Thermanl Analysis. Volume 1.* London and New York: Academic Press.

Mackenzie, R. C., 1959. The classification and nomenclature of clay minerals. *Clay Minerals Bulletin,* pp. 52-66.

Madejova, J., 2003. FTIR techniques in clay mineral studies. *Vibrational Spectroscopy,* Volume 31, pp. 1-10.

Mahmoudi, S., Bennour, A., Srasra, E. & Zargouni, F., 2017. Characterization, firing behavior and ceramic application of clays from the Gabes region in South Tunisia. *Applied Clay Science,* Volume 135, pp. 215-225.

Miller, P. M., 2017. *Continuity and change in Etruscan domestic architecture.* Oxford: Archeopress Publishing LTD.

Minguzzi, V. et al., 1995. Caratterizzazione minero-geochimica e studi termici di varie tipologie di "Concotto" di età etrusca (Marzotto, BO). *Mineralogical et Petrographica acta,* Volume XXXVIII, pp. 219-227.

Mohamed Musthafa, A., Janaki, K. & Velraj, G., 2010. Microscopy, porosimetry and chemical analysis to estimate the firing temperature ofsome archaeological pottery shreds from India. *Microchemical Journal,* Volume 95, pp. 311-314.

Moropoulou, A., Bakolas, A. & Bisbikou, K., 1995. Thermal analysis as a method of characterizing ancient ceramic technologies. *Thermochimica acta,* pp. 743-753.

Mothé, C. G. & Ambrosio, M. C. R., 2007. Process occurring during the sintering of porous ceramic materials by TG/DSC. *Journal of Therman Analysis and Calorimetry,* 87(3), pp. 819-822.

Müller, C. M. et al., 2014. Infrared Attenuated Total Reflectance Spectroscopy: An Innovative Strategy for Analyzing Mineral Components in Energy Relevant Systems. *Scientific Reports,* pp. 1-11.

Munsell, C., 2000. *Munsell soil color charts (Year 2000 Revised Washable Edition).* New Windsor (NY): Munsell Color Company.

Normal, 29/88. *Misura della perdita per evaporazione dell'acqua assorbita del materiale,* Roma: CNR - ICR.

Normal, 7/81. *Assorbimento d'acqua per immersione totale e capacita di imbibizione,* Roma: CNR - ICR.

Orton, C. & Hughes, M., 2013. *Pottery in Archaeology, Second Edition.* New York: Cambridge University Press.

Peinetti, A., 2014. Terra cruda e terra cotta: architettura domestica e attività artigianali.. In: M. Venturino Gambari, ed. *La Memoria del Passato: Castello di Annone tra archeologia e storia 2.* Asti: LineLab, pp. 275-319.

Peinetti, A., 2016. L'analisi tecnologica di resti strutturali in terra: variabilità delle tecniche di costruzione e osservazioni in sezione levigata per la caratterizzazione di concotti e conglomerati architettonici. *IpoTesi di Preistoria,* Volume 8, pp. 103-138.

Pirolandi, L., 2014. *Caratterizzazione chimica e fisica di impasti in terra cruda e proposta di metodologie per il loro consolidamento,* Master's degree thesis in Scienze Chimiche per la Conservazione e il Restauro: Ca' Foscari University of Venice.

Post, J. L. & Borer, L., 2002. Physical properties of selected illites, beidellites and mixed-layer illite–beidellites from southwestern Idaho, and their infrared spectra. *Applied Clay Science,* Volume 22, pp. 77-91.

Ramasamy, V. & Suresh, G., 2009. Mineral Characterization and Crystalline Nature of Quartz. *American-Eurasian Journal of Scientific Research,* 4(2), pp. 103-107.

Ravisankar, R. et al., 2010. Mineralogical Characterization Studies of Ancient Potteries of Tamilnadu, India by FT-IR Spectroscopic Technique. *E-Journal of Chemistry,* 7(S1), pp. S185-S190.

Ravisankar, R. et al., 2010. Mineral analysis of coastal sediment samples of Tuna, Gujarat, India. *Indian Jpurnal of Science and Technology,* 3(7), pp. 774-780.

Ricci, G., 2016. *Archeometric Studies of Historical Ceramic Materials,* PhD thesis in Chemical Science: Ca' Foscari University of Venice.

Sassatelli, G., 1990. *La situazione in Etruria Padana.* Roma, École Française de Rome, pp. 51-100.

Shoval, S., 2003. Using FT-IR spectroscopy for study of calcareous. *Optical Materials,* Volume 24, pp. 117-122.

Shvarzman, A., Kovler, K., Grader, G. & Shter, G., 2003. The effect of dehydroxylation/amorphization degree on pozzolanic activity of kaolinite. *Cement and Concrete Research,* Volume 33, pp. 405-416.

Singh, P. & Sharma, S., 2016. Thermal and spectroscopic characterization of archeological pottery from Ambari, Assam. *Journal of Archaeological Science,* Issue Reports 5, pp. 557-563.

Steingräber, S., 2001. The Process of Urbanization of Etruscan Settlements from the Late Villanovan to the Late Archaic Period (End of the Eighth to the Beginning of the Fifth Century B.C.): Presentation of a Project and Preliminary Results. *Etruscan Studies,* Volume 8, pp. 7-33.

Stevanović, M., 1997. The age of clay: the social dynamics of house destruction. *Journal of anthropological archaeology 16,* pp. 334-395.

Stevenson, C. M. & Gurnick, M., 2016. Structural collapse in kaolinite, montmorillonite and illite clay and its role in the ceramic rehydroxylation dating of low-fired earthenware. *Journal of Archaeological Science,* Volume 69, pp. 54-63.

Tasca, G., 1998. Intonaci e concotti nella preistoria: tecniche di rilevamento e problemi interpretativi. *Archeologia dell'Italia Settentrionale,* Volume 7, pp. 77-87.

Tironi, A., Trezza, M., Irassar, F. & Scian, A., 2012. Thermal treatment of kaolin: effect on the pozzolanic activity. *Procedia Materials Science ,* Volume 1, pp. 343-350.

Torelli, M., 1981. *Storia degli Etruschi.* Bari: Editori Laterza.

Vaculikova, L. & Plevova, E., 2005. Identification of clay minerals and micas in sedimentary rocks. *Acta Geodynamica Geomaterialia,* 2(2 (138)), pp. 167-175.

Velraj, G., Janaki, K., Mohamed Musthafa, A. & Palanivel, R., 2009. Estimation of firing temperature of some archaeological pottery shreds excavated recently in Tamilnadu, India. *Spectrochimica Acta Part A,* Volume 72, pp. 730-733.

Velraj, G., Ramya, R. & Hemamalini, R., 2012. FT-IR spectroscopy, scanning electron microscopy and porosity measurements to determine the firing temperature of ancient megalithic period potteries excavated at Adichanallur in Tamilnadu, South India. *Journal of Molecular Structure,* Volume 1028, pp. 16-21.

Winter, N. A., 2017. Traders and Refugees: Contributions to Etruscan Architecture. *Etruscan Studies,* Volume 20, pp. 123-151.

Zamboni, L., 2016. *Spina città liquida : gli scavi 1977-1981 nell'abitato e i materiali tardo-arcaici e classici.* Rahden: VML Verlag Marie Leidorf.

Zanichelli, n.d. [Online]
Available at: https://dizionaripiu.zanichelli.it/storiadigitale/p/mappastorica/318/la-massima-espansione-degli-etruschi
[Accessed 26 01 2020].

Zemenova, P., Kluozkova, A., Kohoutkova, M. & Kral, R., 2014. Investigation of the first and second dehydroxylation of kaolinite. *Journal of Thermal Analysis and Calorimetry,* Volume 116, pp. 633-639.